6-15-2017

Analysis of an Experimental Space Debris Removal Mission

Krista L.L. Roth

ANALYSIS OF AN EXPERIMENTAL SPACE DEBRIS REMOVAL MISSION

THESIS

Krista L. L. Roth, Capt, USAF

AFIT-ENY-MS-17-J-071

DEPARTMENT OF THE AIR FORCE
AIR UNIVERSITY

AIR FORCE INSTITUTE OF TECHNOLOGY

Wright-Patterson Air Force Base, Ohio

AFIT-ENY-MS-17-J-071

ANALYSIS OF AN EXPERIMENTAL SPACE DEBRIS REMOVAL MISSION

THESIS

Presented to the Faculty

Department of Astronautical Engineering

Graduate School of Engineering and Management

Air Force Institute of Technology

Air University

Air Education and Training Command

In Partial Fulfillment of the Requirements for the

Degree of Master of Science in Astronautical Engineering

Krista L. L. Roth, BS, MS

Capt, USAF

June 2017

AFIT-ENY-MS-17-J-071

ANALYSIS OF AN EXPERIMENTAL SPACE DEBRIS REMOVAL MISSION

THESIS

Krista L. L. Roth, BS, MS
Capt, USAF

Committee Membership:

Eric Swenson, PhD
Chairman

Carl Hartsfield, PhD
Member

Joshuah Hess, Capt, PhD
Member

Abstract

Encountering space debris is an ever-increasing problem in space exploration and exploitation, especially in Low Earth Orbit. While many space-faring governing bodies have attempted to control the orbital lifetime post mission completion of satellites and rocker bodies, objects already in orbit pose a danger to future mission planning. Currently, governments and academic institutions are working to develop missions to remove space debris; however, the proposed missions are typically costly primary missions. This research proposes an alternative to use an upper stage rocket, to be called a chaser, already launching a primary mission near the desired debris as a host for a removal mission. This research models the alternative system as an experimental test concept deploying a target from the Evolved Expendable Launch Vehicle Secondary Payload Adapter ring. A net and tether system is deployed towards the target to capture it, and at the opposite end of the tether is released a drag chute to deorbit the target. Once the capture method is proven with a cooperative body through experimentation, the target can then be an uncooperative piece of space debris of any size. The orbital life of a dead rocket body in an 800 km sun synchronous orbit can theoretically be reduced from approximately 500 years to less than a year using this method. This proposed concept is new in that it is planned as a secondary mission and the majority of the mission components will not separate from the Payload Adapter ring. This research's initial model predictions show feasibility for this new concept.

To my daughter

Acknowledgments

I would like to thank all those who have contributed their time and effort to help me with this thesis. I would especially like to thank my thesis advisor Dr. Eric Swenson for taking me on and working with me to refine my proposed idea. The evolution of the originally proposed concept brought this research from the realm of imagination to a feasible space mission. He continually pushed me to take that extra step in my research to prove how I was proposing something new and innovative to the field and show how my research would have an impact on the space community. I would also like to thank my committee members, Dr. Carl Hartsfield, and Captain Joshuah Hess (PhD) for their support and idea brainstorming sessions. Without their input the refined scope presented in this work would not have been established as early as it was. In addition to the faculty I would also like to thank Captain Stephen Tullino and 1st Lieutenant Joshua Lee for the help with coding issues. Also, I would like to thank the Air Force Research Laboratory for the use of their code as an original idea starting point despite the minimal impact it played in the final product. Finally, I would like to thank my friends and family who have stood by me in my research. They have allowed me to bounce ideas off of them, read my work repeatedly checking for grammar errors and listened to my presentations about my progress. Thank you especially to family for all of your support through this entire process.

Krista L. L. Roth

Table of Contents

Page

List of Figures

Page

List of Tables

Page

Nomenclature

A: State Matrix

A_{chute}: Area of drag chute

a: acceleration

B: Input Matrix

C: Output Matrix

C_d: coefficient of drag

C_r: solar radiation pressure coefficient

D: Direct Transition of feedthrough matrix

d: distance

F: Force

G: Gravitational Constant

g: resultant torque

I: Identity matrix

I: MOI of system

I_{cm}: Current MOI of object before applying parallel axis modification

$I_{parallel\ axis}$: MOI of an object about a parallel axis

$\boldsymbol{J}_{tot}^{B_{CM}}$: Inertia tensor of the total system at the center or mass expressed in the body frame

$\boldsymbol{J}_{obj}^{B_{CM}}$: Inertia tensor of the target object in the body frame

$\boldsymbol{J}_{SC}^{S_{CM}}$: Inertia tensor of the spacecraft in the spacecraft's frame

$\bar{L}$: Angular Momentum Vector

M: mass

m_{SC}: Mass of the spacecraft

$M_{central}$: Mass of the central body

$\bar{p}$: Linear momentum vector

ρ or ρ_o: density

$\boldsymbol{r}^{\frac{B}{A}}$: Vector from B to A

R_E: radius of the earth plus the orbital altitude of the object

t: time

$\bar{u}$: inputs

$\bar{v}$: velocity vector

v: scalar velocity

$\bar{\omega}$: Angular rates vector

x: x axis

$\bar{x}$: state vector

$\bar{x}_o$: initial state vector

y: y axis

$\bar{y}$: outputs

z: z axis

Acronyms

AAReST: Autonomous Assemble of a Reconfigurable Space Telescope

ADCS: Attitude, Determination and Control System

ADR: Active Debris Removal

ARM: Asteroid Redirect Mission

ASAT: Anti-Satellite

ASI: Agenzia Spaziale Italiana

ATLAS: Advanced Telerobotic Actuation System

CADET: Capture and De-Orbiting Technologies

Cal Poly: California Polytechnic State University

CMG: Control Moment Gyroscope

CSD: Canisterized Satellite Dispenser

DARPA: Defense Advanced Research Projects Agency

D-CoNe:

DEOS: Deutsche Orbital Servicing Mission

DICE: Dynamic Ionosphere CubeSat Experiment

DLR: Deutsches Zentrum fur Luft-und Raumfahrt (German Aerospace Center)

DoD: Department of Defense

EELV: Evolved Expendable Launch Vehicle

EPOS: European Proximity Operations Simulator

EPS: Electrical Power Subsystem

ESA: European Space Agency

ESPA: EELV Secondary Payload Adapter

FREND: Front-End Robotics Enabling Near-Term Demonstration

GEO: Geostationary Earth Orbit

GS: Grappling System

ISS: International Space Station

LCROSS: Lunar Crater Observation and Sensing Satellite

LEO: Low Earth Orbit

MOI: Moment of Inertia

MSIS: Mass Spectrometer-Incoherent Scatter Radar

NASA: National Aeronautical and Space Administration

NEO: Near Earth Orbit

ODE: Ordinary Differential Equation

P-POD: Poly Picosatellite Orbital Deployer

RAAN: Right Ascension of the Ascending Node

REDCROC: Research and Development for the Capture and Removal of Orbital Clutter

ROGER: Robotic Geostationary Orbit Restorer

SpaceX: Space Exploration Technologies

STK: Systems Tool Kit

TAKO: Target Collaborativize

TRL: Technology Readiness Level

TSR: Tethered Space Robot

UK: United Kingdom

ULA: United Launch Alliance

UN: United Nations

US: United States

ANALYSIS OF AN EXPERIMENTAL SPACE DEBRIS REMOVAL MISSION

I. Introduction

General Issue

As nations around the world develop new and more advanced technology, they begin to expand further into exploring the benefits of space operations. The number of countries that currently exploit space has grown significantly in the last few decades with an expectation for it to continue [1]. With the increased interest and use from governments and private companies, the amount of material going into space has been steadily rising [2]. As a result of the increase in material, there is an increased chance of collisions, that subsequently create additional debris. Of the greatest concern is low Earth orbit (LEO) where the majority of satellites currently orbiting Earth are located. J C Liou predicted that eventually LEO will be unusable due to the amount of debris from exponentially rising collisions as predicted by Kessler and Cour-Palais in 1978 [2]. Because of this startling possibility, countries have begun instituting limitations on how long objects are allowed to remain in orbit after their useful life. Several organizations worldwide have also started initiatives to look at reducing the amount of debris and dead objects that currently reside in LEO [3].

The efforts to reduce space debris to date have been more theoretical with ground based testing rather than routine missions that aim to capture and remove debris such as e.Deorbit by the European Space Agency (ESA) [3]. There are several barriers to the space debris removal mission concept. Chief among the afore mentioned barriers is the large cost to build and launch a satellite that does not serve a purpose for the nation or corporation beyond cleaning up space. To make the space debris reduction objective more appealing, a mission concept that is capable of utilizing a low cost satellite or that can make use of currently launching upper stages already

planning to re-enter can be explored. Presently some universities and national organizations, such as the ESA, Defense Advanced Research Projects Agency (DARPA) and University of Colorado Boulder, are exploring small and large satellite implementations [3]. An area that could provide immense benefit to the community is the use of upper stages as a carrier vehicle for a device capable of capturing large debris. With the removal of large debris from highly desirable orbits, LEO can be made usable without the fear of a loss of capability.

Problem Statement

The purpose of this study is to model and create a simulation of a proposed experimental system that can be attached to an United Launch Alliance (ULA) Atlas V (and future proposed Vulcan) upper stage, the single engine Centaur rocket that is capable of decreasing the orbital life of space debris. This thesis presents a methodology for the use of a Centaur, from here on out to be referred to as the chaser, via an externally mounted control system to aid in a close approach maneuver. The mounted system will release a cooperative target, deploy a net to capture the target and then deorbit the target using a drag chute. Another aspect analyzed is the possibility to scale up the target to the same size as the chaser and still deorbit within 25 years of capture. Additional problems investigated included a look at the total benefit that is gained from this type of implementation and a look at safety precautions to be undertaken in the implementation of the system and mission to minimize the risk of creating additional debris.

Research Question/Hypothesis

In this research, the use of a Centaur and Evolved Expendable Launch Vehicle (EELV) Secondary Payload Adapter (ESPA) ring as a host for a debris removal mission is studied.

Modeling will be conducted to determine feasibility of the design using a self-deployed target from the ESPA ring to be captured by a full size net and tether system which will then be de-orbited by an independent drag chute released from the ESPA ring. The complete dynamics of this system will be modeled to determine feasibility of the proposed mission. Additionally in this research, the benefit gained for a non-cooperative dead rocket body using the proposed modeled system will be studied.

The goal of this study is that a series of boxes mounted to an ESPA ring on a Centaur are capable of capturing a target and reducing its orbital lifetime.

Research Focus

The focus of this study will be the modeling and simulation of the mission from post close-approach maneuvers by the chaser until the deorbit of the self-deployed target. The use of an ESPA ring as the chaser and deploying the drag chute for the target to de-orbit are novel in the area of debris removal research while the use of net and tether systems in combination with a drag chute is not. The focus will be to study the feasibility of the complete proposed system rather than fine detail of the net and tether system.

The ideal use of the system is to capture a dead rocket body; however, initial modeling is done on a concept mission using a self-deployed 27U CubeSat as a target. The initial orbit of both the chaser and target would be such that both would deorbit within the required 25 years without further assistance.

Methodology

This study will evaluate and estimate the current lifetimes of a dead rocket body at varying altitudes and inclinations and the amount of delta V is required to achieve the desired final altitudes. The proposed final mission concept is to deorbit a dead rocket body using the ESPA as a host. The presented research will be modeled using a self-deployed target instead of making a rendezvous with existing orbital debris in an orbit determined safe in terms of orbital lifetime for all components of the mission. After the deployment of the target, a net and tether system will be deployed followed by a drag chute. The capture system will deorbit the target independent of the chaser.

Assumptions/Limitations

Several constraints and limitations have been placed on the scope of the included study. The politics of space debris removal will not be addressed. The problem is constrained to looking at only using a current Centaur single engine upper stage rocket as the chaser. The two-engine variation of the Centaur was not considered for this research. The target during the orbital lifetime analysis is a second Centaur single engine upper stage and during the modeling portion is a deployed 27U CubeSat originating from the chaser. The chaser rocket is assumed to be capable of reaching the desired orbit after releasing its primary payload with residual fuel needed to complete at least a partial re-entry burn and completing the close approach maneuvers. The position and velocity are only modeled locally to the system. The specifications of the net, specifically the dimensions and weights of the components, to be employed by the system have been determined by previous work and are sufficient to capture the self-deployed target. A scaled up version from the same research would be capable of capturing the dead rocket body. The

research looks at the system rather than details of net deployment design and dynamics which have been studied extensively to date.

II. Literature Review

Chapter Overview

The rate at which debris is being deposited into LEO (less than 3,000 km in altitude), has been increased steadily since spaceflight began [4]. This is a factor of the continually growing space community attempting to utilize the space and the slow rate of orbital decay of objects currently occupying the space. To prevent making space inaccessible due to the growing debris field, this author and others developing ADR satellites such as e.Deorbit believe action has to be taken early to start eliminating large objects [5] [6]. Several mission concepts have been proposed over the years and a few have made it to the design and testing phase [3] [7]. The greatest challenge to correcting the orbital debris problem is not imposing rules and regulations on currently launching spacecraft, but rather finding a cost effective solution to correct the already existing on-orbit issue of large objects posing a risk of creating a cascade effect of more debris [8]. This chapter will cover what active debris removal (ADR) entails, current technologies being researched or developed for use in ADR, modeling done with net and tether technology and hosted payloads on an ESPA ring.

Description

According to Schmitz et al. and the ESA, there exist over 17,000 identified objects larger than 5 to 10 cm in LEO with only 1,200 of those being active satellites [9]. It has been reported [5] that in order to keep LEO usable for the foreseeable future, 5 to 10 large objects need to be removed every year. The reduction in debris can reduce the possibility of the cascading of debris collisions in high risk regions such as sun-synchronous orbits [9]. The United Nations (UN) report [10] defines large debris as anything over 10 cm in size. Currently, there exists no

economically feasible option for the removal of large space debris by either a space or ground based platform [11]. The lack of economically feasible options or secondary missions creates a large barrier for most countries to creating and launching space debris removal missions.

The National Aeronautics Space Administration (NASA) has established guidelines on debris analysis required prior to the launch of any mission, and these guidelines have subsequently been adopted by the United States (US) Government for all Department of Defense (DoD) Launches as well. The most constraining factor in the guidelines is that all spent rocket stages and satellites at the end of their life must be moved to a pre-determined parking orbit, such as the Geostationary Earth Orbit (GEO) parking orbit beyond the GEO belt, or de-orbit within 25 years after the end of their mission [12]. The contributing factors to the growing debris issue include long de-orbit times for unassisted debris, increasing use of space, collisions, and anti-satellite testing (ASAT) as conducted by both the US and China [13]. There is no international treaty mandating how to handle or minimize space debris by the international community, however there were non-binding guidelines published by the United Nations in 2010 [14]. As an example, the 25-year limit used by the US and the ESA, is only followed by 80% of upper stage rocket bodies and 60% of satellites [15]. To mitigate the problem, institutions from across the globe have been researching for years different approaches to reducing the amount of debris currently in orbit. Ground based systems such as lasers that are intended to pulverize 1 to 10 cm debris could potentially reduce the small debris in LEO by up to 23%; however, the issue of creating additional untrackable debris exists with this method [11]. Also under development is a collection plate for the capture of microscopic debris; however, this type of debris is not the most appealing for capture targets due to the limited risk to active systems they currently pose [16]. To adequately address the debris issue, a large-scale mission whose objective is large target objects

such as spent rocket bodies currently appears to be the only practical option available. Large-scale missions that have been proposed currently require larger satellites with higher price tags, such as e.Deorbit's mission cost ceiling of 150 million Euros, and complexity for what many see as a disposable satellite offering no use to furthering science or products for the commercial industry [17].

Relevant Research

Currently, the ESA has started a Clean Space Initiative in an effort to bring awareness to the issue with space debris and to promote research to find missions capable of assisting in the active removal of debris [17]. The ESA states that "the most effective short-term" solution to the space debris problem is the "prevention of in-orbit explosions" [17]. However, this does not address a long-term solution that would require debris removal in order to reach a "safe-level" for the debris environment [17]. To the extent of the literature review, not addressed in any of the research is the impact of large projects such as Elon Musk's SpaceX project to provide global satellite internet with a 4,000 satellite LEO based constellation [18]. There have been several studies into possible space debris removal missions and some studies into combined body dynamics and detailed modeling of the different elements of a debris removal mission [2] [7] [9] [11] [18-24]. There is no current research on using a Centaur and ESPA ring to host a secondary debris removal mission capable of capturing a dead rocket body.

Impact of Debris Removal Systems

The following section will cover why debris removal missions are needed and why this research is relevant to the current space environment. The biggest question facing the world

today concerning fixing the space debris problem is whether active space debris removal missions will have any impact or is it already too late to fix the problem with our current levels of technology. NASA and the DoD were directed by President Obama in 2010 to "pursue research and development of technologies and techniques… to mitigate and remove on-orbit debris, reduce hazards, and increase understanding of the current and future debris environment" [2]. With this direction, NASA conducted a sensitivity study to determine the impact of ADR on the stabilization of the LEO debris environment [2]**.** The current mitigation strategy did not qualify as active debris removal and for the purposes of the study varying levels of debris removal efforts were considered against a control of no removal and a rate of growth commensurate with the current level of launches as shown in Figure 1 [2].

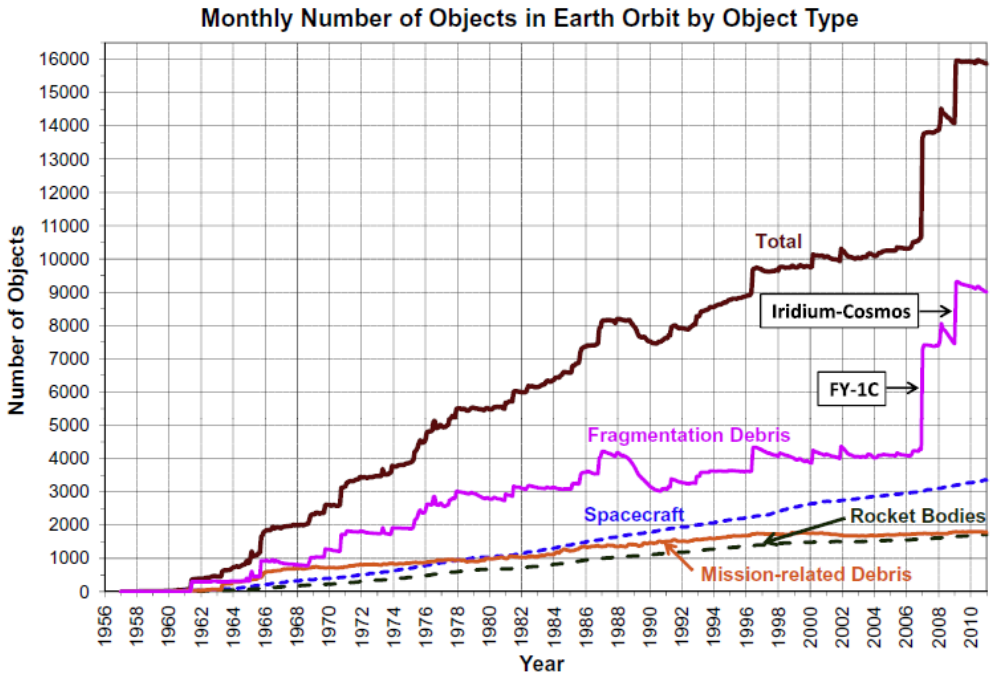

Figure 1: Monthly increase of objects in space. Pointed out are the FY-1C ASAT test and the Iridium/Cosmos collision spikes [2]

In 2010 40% of the total 5900 tons of mass in orbit resides in LEO in three different concentrations (600, 800 and 1000 km) most of which are rocket bodies (at 800 and 1000 km) and spacecraft (at 600 km) as seen in Figure 2 [2].

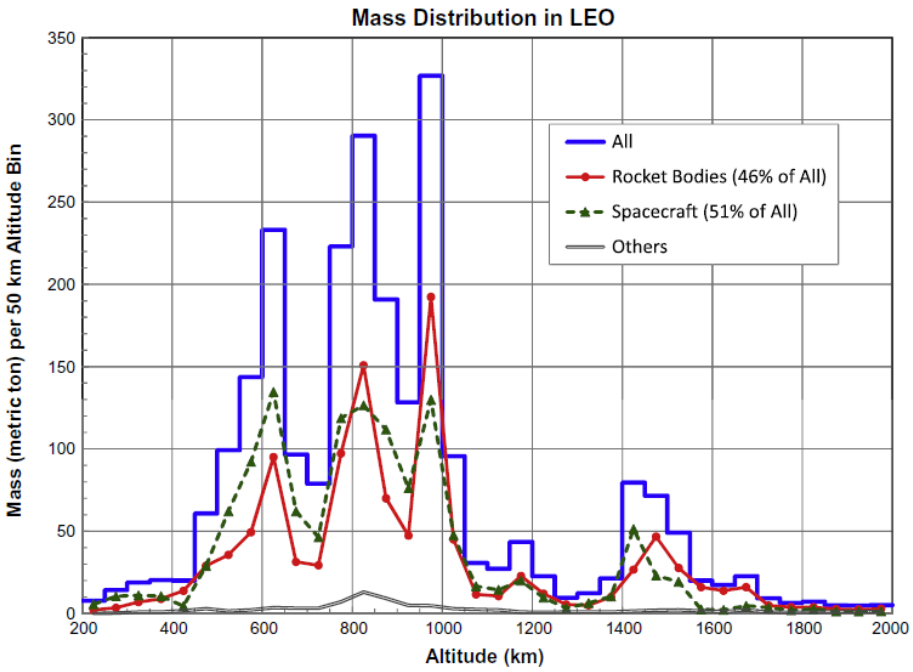

Figure 2: Mass distribution in LEO. (The International Space Station is not included in the distribution) [2]

Liou showed that in the next 200 years there would be a 60% increase in the mass of the LEO debris environment, however, not addressed was at what point LEO would no longer be useable as it currently is, or passed through with either signals or spacecraft [2]. After a study into current technology, NASA predicted that between the years 2020 and 2060, technology will be advanced enough to conduct ADR missions. However, waiting towards the end of this window results in approximately 2,000 more objects due to collisions in the same timeframe [2]. Of note, the study stated that limiting to a narrow inclination range might not be the most efficient way to control the debris population at a given altitude [2]. Finally, the study identified

the top 500 targets with the highest mass and collision probabilities by altitude and inclination that included Cosmos, SL-3, SL-8 and SL-16 rocket bodies and Envisat ranging from 1,000 to 8,300 kg [2]. This study did not address why going after the largest objects over just those objectives with high collision probabilities or damage potentials was the preferable approach. If repeated, the study may focus more on damage potentials from collisions, however, this would be a simulation and computing intensive effort and may not be a cost-effective approach for mission planning purposes.

Current and Planned Space Debris Removal Missions

In this section, current research and proposed space debris missions are discussed including different approaches to removing debris and the pros and cons of each method to the overall mission success probability. All of these approaches were considered prior to final selection for this research in an attempt to determine the area where the greatest degree of impact to the field could be made. In looking at the variety of debris removal missions today, they fall into several different categories of removal types including [3]:

- Stiff Connection Capturing: tentacles, and single/multiple robotic arms
- Flexible Connection Capturing: nets, tether grippers, and harpoons (nets are studied in this research)
- Drag augmentation systems (studied in this research)
- Electro-dynamic tethers
- Solar radiation force
- Contactless and contact removal methods

All of these debris removal approaches come with advantages and disadvantages to their use. Next systems that currently have work in progress, including stiff and flexible connection capturing and drag augmentation systems, will be discussed.

Stiff connection capturing methods are currently being developed by Aviospace, German Aerospace Center (aka Deutsches Zentrum für Luft- und Raumfahrt or DLR), DARPA, ESA, Japan, and the United Kingdom (UK) [3] [19]. Within this category are tentacle and robotic arm style capturing devices. The difference between the two is that tentacles are flexible appendages that can "embrace" the debris at multiple points rather than latching on to a single point as done by robotic arms [3]. Tentacle operations can be performed with or without a robotic arm assist in the capture of the target [3]. The advantages of tentacle systems include the ease of test and higher Technology Readiness Level (TRL); however, it has the issue of being a higher cost, mass, volume and hazardousness level project [3]. As a result of these factors, tentacle systems are not as appealing for debris removal missions unless they could be incorporated into a satellite that could dispose of multiple pieces of debris per chaser satellite, reducing the cost per piece of debris removed. Examples of satellites and test systems currently under work are shown in Figure 3.

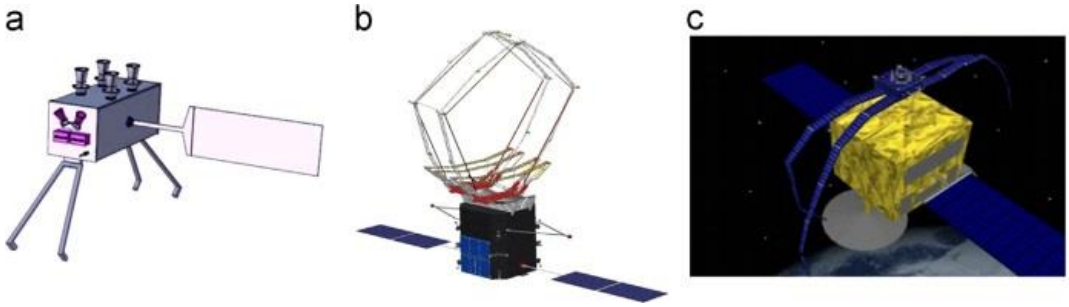

Figure 3: Examples of current tentacle capture satellites (a) e.Deorbit by ESA (b) Capture and De-Orbiting Technologies (CADET) by Aviospace (c) Target Collaborativize (TAKO) Flyer/Gripper by Japan [3] [20]

Of these systems, the CADET satellite by Aviospace is the closest to on-orbit testing with ground testing having occurred in November 2015, which is a year after the original predicted launch date of 2014 [3] [7]. The delays may in part be due to the relatively low TRLs of tentacles such as CADET advertising a starting TRL of 2 and rising to 4 over the course of development [21]. The other type of stiff arm capturing method, the robotic arm, has a much higher TRL and space flight history as seen on the International Space Station (ISS) and the Space Shuttle. For these reasons, the tentacle type of capture method is not ideal for a mission designed to be low cost (need to do extensive testing and development still exists) and employed in the near future (which would require a TRL of 6 or higher for an active mission rather than demonstration) to be considered.

Robotic arms can be used as a single arm or multiple arm cooperative system. These systems would have a much more appealing concept to a near term mission than the previous concept; however, for reasons explained below are robotic arms are not ideal for the proposed research. While the cost is lower for a single arm system, a satellite is more flexible with a multiple arm system [3]. These systems are typically very easy to test on the ground and have a high TRL; however, rendezvous and docking maneuver are required as well as a point on the target to grapple [3]. Determination of the grappling point is one of the larger issues when the robotic arm approach is considered. One must consider the fact that space debris is tumbling in what can be seen as an unpredictable way and may or may not be of a known configuration. Also of note is that once the chaser satellite attaches to the target an “impact influence” is experienced that will affect the overall dynamics of the system creating the need to plan for an optimal time and position to perform the capture with respect to a deorbit plan [3]. Examples of current single arm satellites and ground test systems are shown in Figure 4.

Figure 4: Single Robotic Arm Capture Satellites. (a) Deutsche Orbital Servicing Mission (DEOS) by DLR (b) European Proximity Operations Simulator (EPOS) by DLR and (c) Front-End Robotics Enabling Near-Term Demonstration (FREND) by DARPA [3]

The EPOS system was designed as a ground based test facility for hardware-in-the-loop testing of the behavior of satellites during their docking and capture phases of their missions [3]. The only current multiple arm satellite in development is the Advanced Telerobotic Actuation System (ATLAS) that is being designed in the UK[3]. Multiple arm systems are less cost effective with more mass and complexity than their single arm counterparts that are equally capable of performing the same mission, making them a less desirable first choice for debris removal missions [3]. Overall, the incorporation of any stiff connection capturing method would require a large amount of money as well as a larger satellite capable of housing the battery and computing power required to perform their missions. These missions would not be suitable for a hosted mission on an ESPA ring.

Of greatest interest are flexible connection capturing systems for a hosted mission concept which are being evaluated as a part of this research. Flexible connection capturing systems can be used in smaller scale satellites to some degree unlike most stiff connection capturing systems. The largest advantage of most of these systems is that they do not require a precise rendezvous with the target. The tether-gripper approach is the exception as it does require a grappling point [3]. The focus of most research in this area has been done on net capturing

systems. Their obvious advantages include a “larger capturing distance,” up to 100 m seen to date, that reduces the requirements on precision and compatibility with different size debris targets, however, the nets can be hard to control, are difficult to test on the ground and have a risk of critical oscillations [3] [5]. Net capturing systems have varying dimensions capable of capturing different sizes and amounts of debris. Current systems under development are shown in Figure 5.

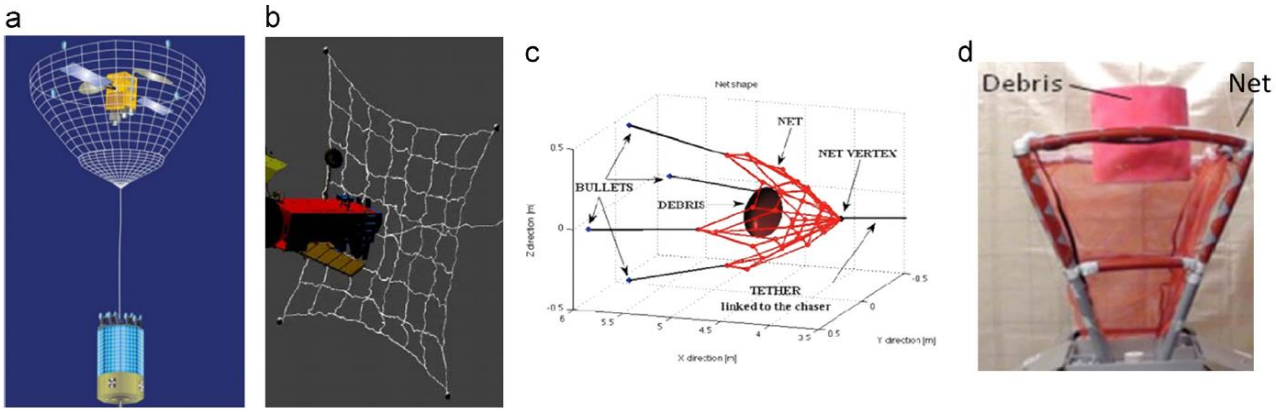

Figure 5: Current net capturing satellites. (a) Robotic Geostationary Orbit Restorer (ROGER) (focused on GEO mitigation) (b) e.Deorbit by the ESA (c) Debris Collecting Net (D-CoNe) by Italy and (d) Research and Development for the Capture and Removal of Orbital Clutter (REDCROC) by University of Colorado at Boulder [3]

The basic concept of a net capturing device is to shoot four weights attached to a net from a spring system on the main body of the chaser satellite. They are typically modeled as a spring-mass system in simulators [3]. The REDCROC satellite takes a slightly different approach with creating an inflatable arm net [22]. After capture, it takes approximately 365 days to deorbit the debris from 900 km with an assist from a drag augmentation balloon, and only one piece of debris can be targeted per satellite launched [22]. The design shows more promise with its size than many other systems, being approximately 1.78 x 1.17 x 2.01 m^3 in size, with the intent to

launch 10 satellites at once that all perform transfer orbits to intended debris targets [22]. In its published configuration, it would be limited on the size of debris it could capture and may not be able to target large spent rocket bodies. A proposed net system by Benvenuto and Lavagna is 36 m x 36 m in size and would be capable of capturing debris up to 8000 kg with a flexible appendage such as solar panel [23]. Benvenuto and Lavagna's work is used for sizing the net in this research.

While net capturing systems are the more popular of the flexible connection capture concepts, there are two other concepts currently being explored, a tether-gripper and a harpoon, that should be discussed for completeness of the research. A tether-gripper is similar to a net in that it allows for a larger capturing distance with lower mass and cost; however, it does require a grappling point for the gripper portion of the system [3]. The configuration requires that the tether must always be under tension to avoid the possibility of a collision between the target and chaser during reentry [3]. Overall, the system has a lower reliability than other alternatives and is not well understood [3]. Currently the only examples of a tether-gripper system are ROGER by the ESA and Tethered Space Robot (TSR) by China [3] [24]. The harpoon system eliminates the need for a gripper point and is compatible with multiple target types, however, also has the disadvantage of potentially causing additional debris either by creating fragments due to the capture or compromising the target sufficiently to cause breakup [3]. Due to the nature of the system, it is not compatible with high tumbling rate targets but Astrium and ESA are still working on Grappling System (GS) and e.Deorbit respectively to demonstrate a harpoon system [3]. Overall, the harpoon method has a higher TRL and lower cost when compared to the net capture method, as well as it being relatively easy to test on the ground which could bring it to the front in a competition between the two [3]. The simplicity of many of the flexible connection

capture methods and low cost make these systems ideal concepts for implementation on a much smaller satellite with the intent to reduce costs.

Other than the previously mentioned methods, the most promising removal method is a drag augmentation system which increases the area-to-mass ratio of the debris to increase its atmospheric drag [3]. This method can be used in conjunction with other methods and is being considered as a part of this research for deorbit purposes. This approach can be used in conjunction with other approaches as shown by the University of Colorado's REDCROC satellite or independently [22]. Several different tactics have been proposed for this type of mission such as spraying a target with foam and turning it into a large foam ball, inflating a large ball-like envelope on either the chaser satellite or directly on the target or a fiber-based substance extruded from a heat source to wrap the target much like the foam ball approach [3]. These approaches are seen in Figure 6.

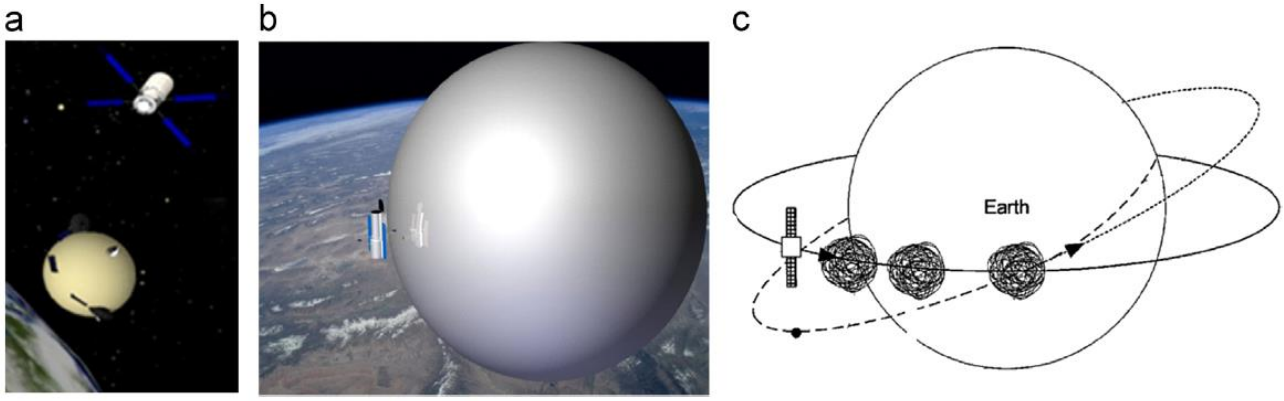

Figure 6: Drag augmentation mission concepts. (a) foam method (b) inflated balloon method (c) fiber-based method [3]

Other than the previously mentioned application being used by REDCROC, these methods are not being explored for a currently under development mission. A concept that is starting to

become more prevalent is the use of a drag chute or drag sail to deorbit satellites in LEO at the end of mission life [25] [26].

A feature that most of the satellites currently in development for space debris removal missions have in common is the highest priority targets to go after first. A study was conducted by Agenzia Spaziale Italiana (ASI) in Italy that determined which rocket bodies would be the best to remove first for the greatest impact for the cost of the chaser satellite [9]. Of greatest interest appears to be bodies in either 800 km orbits with an inclination of 99 degrees or 1,000 km orbits with an inclination of 82 degrees [9]. Between the two orbits there are 41 bodies ranging from 65 to 3,800 kg in the first and 317 bodies ranging from 500 to 1,500 kg in the second [9]. In conjunction with this study a proposed satellite mission would attach Thruster De-Orbiting Kits to dead rocket bodies using multiple robotic arms to capture and attach the kit as shown in Figure 7 [9].

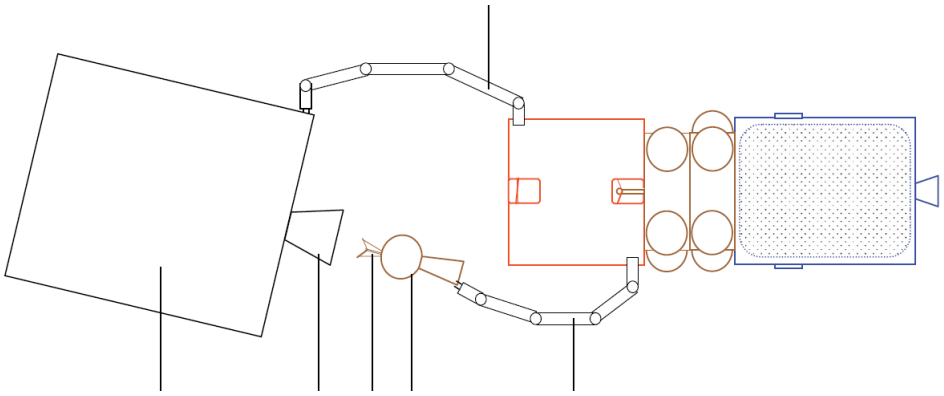

Figure 7: Modular debris removal satellite placing Thruster De-Orbiting kits onto a piece of debris. For rough sizing purposes the red box is 1.5x1.5x1.5 meters cubed [9]

The satellite would need to be resupplied up to 8 times to accomplish a 7-year mission life with 5 targets per year but would have a modular design to simplify the resupply [9]. The new attached thrusters would put the debris into a “fast decay” orbit that would have an altitude that will have

an apogee below 700 km within 12 months of firing the thruster [9]. The sample mission currently does not have a name or expected launch date as of the publishing of the article in 2011 [9]. Overall, most missions currently being explored involve applications of higher TRL technology with the intent to go after multiple targets during the mission life. None of the proposed missions to date have mentioned possible side missions or being a secondary payload to a different primary mission.

Current Research in Modeling Debris Removal

In order to make a debris mission possible that involves touching a target object in some way either through a ranged catching object such as a net or a rendezvous with robotic arms, the dynamics of the combined system could be drastically different that those of the original system. Using the assumption that the targets are all non-cooperative, then all control must be provided by the chaser satellite. With this in mind, potentially none of the attitude controls will be in ideal locations for both the chaser satellite alone as well as the combined system, thus a realistic tradeoff in placement must be made.

To combat some of these issues, nonlinear attitude and control algorithms are under development that allow for the optimal control of the combined system while having the placement of the attitude control systems within the chaser satellite be in optimal positions for the actual rendezvous [27]. The specific intent of the research was to take the combined system case to a logical extreme where a smaller chaser satellite would attach to and direct a significantly larger object such as asteroid or boulder [27]. The control strategy was developed in conjunction with the NASA proposed Asteroid Redirect Mission (ARM) which intends to

"capture a near Earth orbit (NEO) asteroid or to pick up a boulder from some bigger asteroid and transport to the Earth-moon system" as shown in Figure 8 [27].

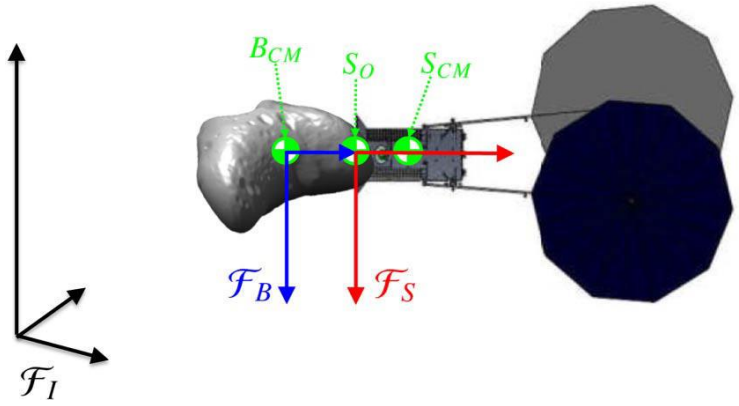

Figure 8: ARM spacecraft with captured asteroid. The displayed frames are the inertial, F_I, body fixed, F_B, to the target and satellite fixed, F_S. Also shown are the center of mass of the body, B_{CM}, and the satellite, S_{CM}, and the satellite origin, S_O [27]

The proposed control law promises exponential convergence of tracking errors and has been demonstrated with numerical simulations using the ARM concept and is related to the tracking control law for Euler-Lagrangian systems [27]. Of the greatest importance to the relevance of the current research are the non-cooperative state of the target and the uncertainty of the target's size and shape prior to mission launch [27]. The combined inertial tensor of the entire system is expressed in the body frame of the captured object as

$$J_{tot}^{B_{CM}} = J_{obj}^{B_{CM}} + J_{SC}^{S_{CM}} + m_{SC}\left[\left(r^{\frac{S_{CM}}{B_{CM}}}\right)^T\left(r^{\frac{S_{CM}}{B_{CM}}}\right)I - \left(r^{\frac{S_{CM}}{B_{CM}}}\right)\left(r^{\frac{S_{CM}}{B_{CM}}}\right)^T\right] \quad (1)$$

The $\left(r^{\frac{S_{CM}}{B_{CM}}}\right) = \left(r^{\frac{S_{CM}}{S_O}}\right) + \left(r^{\frac{S_O}{B_{CM}}}\right)$ term and $\left(r^{\frac{S_{CM}}{S_O}}\right)$ term are the known vectors from the spacecraft origin, fixed at the joining point between the captured body and the spacecraft, to the spacecraft center of mass [27]. Mass is that of the spacecraft and does not account for the mass of the captured object [27]. This equation could potentially be modified for further work with known capture objects and projected weights to reduce some of the errors and uncertainties. The system could also be improved by going after known targets such as recently launched rocket bodies that are not projected to re-enter within the 25-year limit. Not addressed in the proposed research was how to actually conduct the rendezvous with the target and how much the target could be working against the chaser satellite with an initial erratic tumbling motion.

Other modeling work that has been done to date includes extensive work on modeling the detailed mechanics of a net capture device. While D-CoNe modeled their net to include the net, debris, net vertex and bullets, bullets were modeled as point masses attached to the net via a tether as seen in Figure 9.

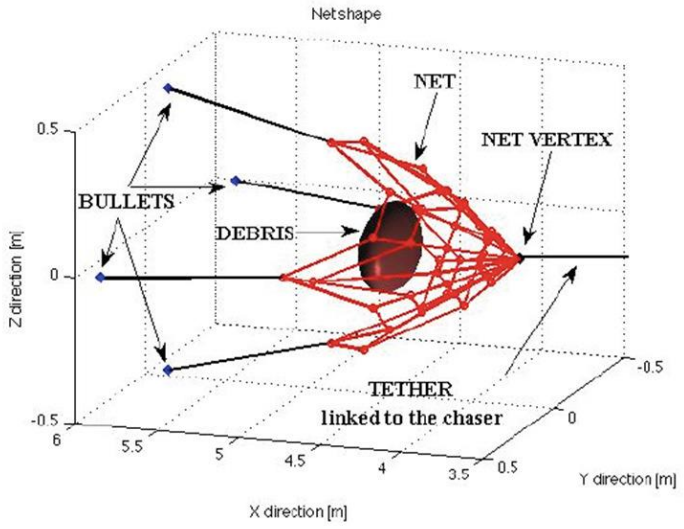

Figure 9: D-CoNe concept model of net capture of ovoid shaped debris [23]

Benvenuto and Lavagna conducted detailed analysis into the net itself using different size nets, weights and mesh sizes. They modeled their nets considering each detail of the mesh making it a lumped spring-mass model to show the flexibility of the net however it also comes with a very large number of constraints [23]. An image of how one section of mess is modeled is seen in Figure 10

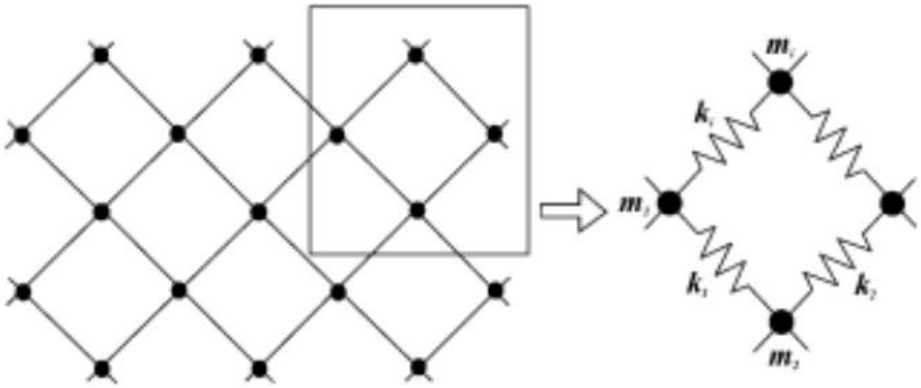

Figure 10: Net mesh modeling for a lumped spring-mass model as done by Benvenuto and Lavagna [23]

The only modeling published that was found to include the exact dimensions of a bullet that was not a point mass or spherical was e.Deorbit [28]. e.Deorbit used a cylindrical mass similar to the one proposed by Benvenuto and Lavagna in their research. Each mass was similar in size to a marker pen and propelled at an angle causing the net to open as it traversed the distance to the desired target and then become entangled within the net after closing around the target [28].

New Debris Removal System Concepts

Most published research on debris removal evaluates small to large satellites to capture space debris. One possibility is the use of a CubeSat as a chaser, while another would be the use

of the ESPA ring attached to a Centaur Rocket. Neither approach has been proposed to date as a viable mission concept however CubeSats have been proposed as a testbed for some of the technologies including the net and tether systems as well as the harpoon and drag sails [26]. Both of these possibilities would expand the available trade space for designers to reduce costs and create secondary payloads.

A 1U CubeSat is nominally defined as a 10 cm cubed body that typically weighs up to 1.33 kg [29]. Each of the nominal cubes can be combined to create a larger CubeSat in several standard sizes including 3U (1x3x1 cubes), 6U (2x3x1 cubes), 12U (2x3x2 cubes), 27U (3x3x3 cubes) [30]. The actual final dimensions of the larger CubeSats exceed the nominal dimensions provided by their labels. Variations on these sizes have been seen, such as the Dynamic Ionosphere CubeSat Experiment (DICE) and the Autonomous Assemble of a Reconfigurable Space Telescope (AAReST) [31] [32]. However, they are typically designed to fit within preexisting launch containers such as Planetary Systems Corporation's (PSC) Canisterized Satellite Dispenser (CSD) or California Polytechnic State University's (Cal Poly) Poly Picosatellite Orbital Deployer (P-POD) [30] [29]. With the size of a CubeSat in mind, the space required to put both a capture device such as a net, as well as a deorbit device such as a drag augmentation system, there is little space remaining for standard satellite components such as the attitude and determination control subsystem (ADCS) and electrical power subsystem (EPS). With the requirement to be able to capture and control a combined body CubeSat and spent rocket body, an oversized ADCS most likely would be required compared to a standard CubeSat ADCS. Currently existing modeling for net capture device deployment, capture and spacecraft dynamics, such as created for e.Deorbit or ROGER, could potentially be modified for a CubeSat application [3]. e.Deorbit researchers have shown that testing such a net can be conducted on a

special aircraft that flies a parabolic orbit to simulate microgravity for testing of the net deployment and capture of a stationary object [28]. The existing modeling for such a system could be scaled up to show a larger target and net design.

The concept evaluated in this presented research would be to create a mission that never detaches from a Centaur ESPA ring. Only one similar mission has been conducted to date. NASA performed a mission using the ESPA as a host on the Lunar Crater Observation and Sensing Satellite (LCROSS) Mission to the moon [33]. Several control and data collection panels were attached to the connection points of the ESPA ring as seen in Figure 11.

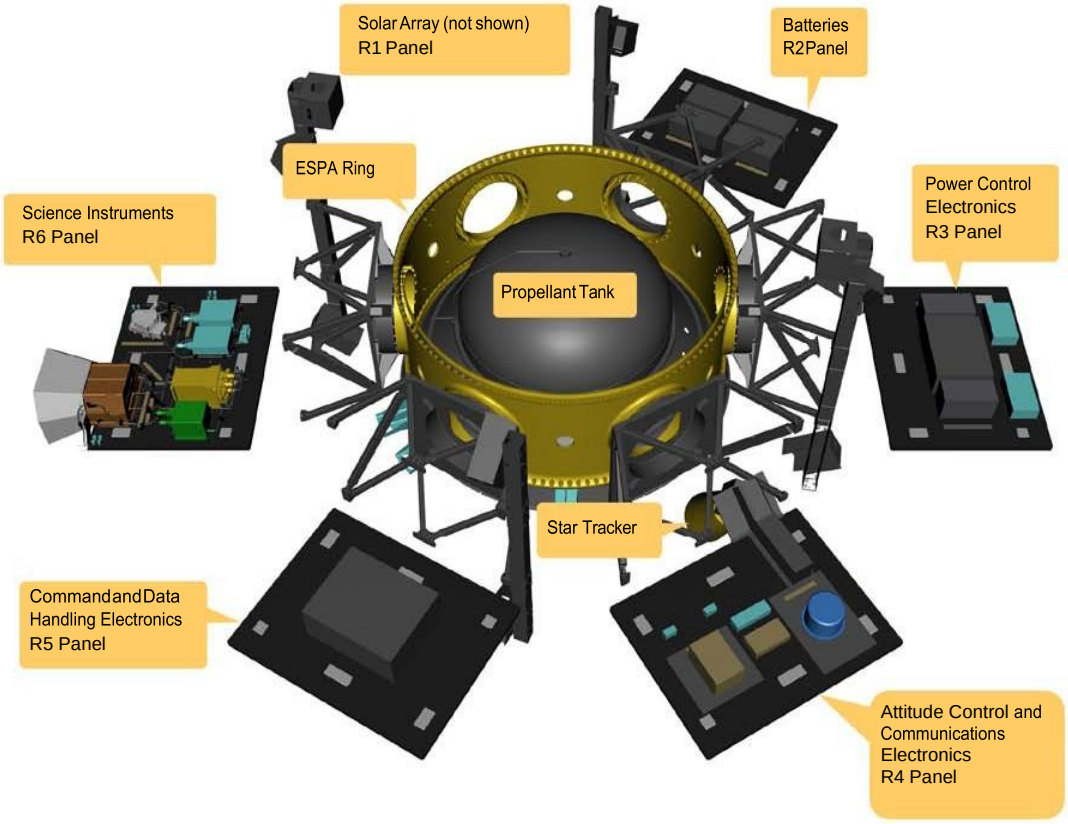

Figure 11: LCROSS Spacecraft ESPA Ring Configuration [31]

The main propulsion, communications and power could be supplied from the Centaur rather than needing to provide an independent source onboard the satellite. A net and tether system could be

added to an ESPA ring location as well as additional ADCS at another location. The added ADCS would provide finer control that is required for matching the rotation of a target as well as detumbling the target. An additional propulsion system may be necessary for close approach/rendezvous operations, however, using one or two of the six locations on the ESPA ring would not pose a problem for this. The only requirement for this approach would be having a primary mission going near the desired location for the debris removal. The reasoning behind this is that additional fuel will be needed by the Centaur to perform the orbit change to get to the rendezvous orbit and conduct a potentially larger deorbit burn than would have previously been required. The primary mission would require the secondary payload to ensure there are no risks associated with the equipment added to the ESPA ring. There is to the risk to the secondary payload after the primary payload deploys due to the repeated starts and stops of the Centaur main engine or a need to carry a secondary engine. A potential benefit, however, is the possibility to add more than one net and tether system to the ESPA ring to allow either multiple attempts at the same target or, depending on the remaining Centaur fuel, the ability to go after multiple targets.

A similar project to the proposed test is the mission in 2016 of RemoveDEBRIS by the University of Surrey [26]. While still only a concept tester for the different types of technologies, it launched a self-deployed CubeSat that would then be captured again. They used a net and tether system as well as a harpoon designed not to cause additional debris. A drag sail was planned to be attached to the main body to burn it up however it was not clarified if it was also used on the target. The updated mission timeline will not have it launching until 2017 from the ISS [25]. This mission however is not meant to be a demonstration of full scale net or drag sail technologies, rather a concept mission for the types of removal methods [26]. Even the small-

scale mission is forecast to cost about 13 million Euros with the full-scale mission being significantly more. The biggest difference in the RemoveDEBRIS mission and the proposed research is the lack of testing full scale and not requiring an independent satellite to carry the debris removal method.

Summary

Extensive work has been done to date to design systems to attempt to solve the space debris in LEO; however, there have not been any missions launched and showing flight heritage of the technologies. Two missions are currently scheduled but were delayed from their originally published launch dates, RemoveDEBRIS in 2017 and e.Deorbit in 2023 [25] [6]. According to Shan et al. the most promising options are in robotics and net capture devices [3]. The major limiting factor in all proposed missions to date is limited impact on debris removal for large amounts of money on potentially single mission spacecraft. The largest gap in current technologies is designing a space debris removal spacecraft that can fly as a secondary payload or with a secondary payload. By taking a secondary mission approach to the issue, a cost reduction, or sharing, can be achieved making the appeal of conducting these types of missions higher and thus cleanup of LEO more likely before it becomes unusable. If a design could be achieved to accomplish this mission at a lower cost, governments around the world would be more amenable to conducting debris removal missions in addition to leveeing guidance on debris lifetime for future missions.

III. Methodology

Chapter Overview

In this chapter, the methodology of the modeling will be discussed. Explained in detail will be the equations used for modeling the chaser capturing the target with a net tether system and releasing a drag chute. Also to be discussed are the chosen parameters and the modeling of the orbital lifetime calculations for the dead rocket body target scenario.

Target Orbital Life

The orbital life of an object is primarily dependent upon its cross-sectional area, mass, mass moment of inertia and area exposed to the sun. While some of these do not change with orientation, such as mass and mass moment of inertia if the body is non-deformable, others, such as the cross-sectional area and area exposed to the sun, are highly dependent on orientation and could change rapidly if an object were tumbling. Orbital lifetimes also depend on inclination and altitude. To predict the lifetime of the chaser, the approximate dimensions were used for a Single Engine Rocket Centaur upper stage from the NASA Technical Memorandum for the Centaur [34]. In Table 1, there are the specifications used for the single rocket system including the Centaur specifications and orbital parameters.

Table 1: Centaur Specifications and Mission Orbital Parameters

Mass [34]	2247 kg			
Radius [34]	3.05 m			
Height [34]	12.68 m			
Moment of Inertia (MOI) (estimated)	35300	0	0	$kg*m^2$
	0	35300	0	
	0	0	10400	
Altitude	300-1100 km			
Eccentricity	0			
Inclination	0-92 degrees			

The mass moment of inertia is approximated using Eq. (2) using the NASA information and the approximation of a cylinder [34].

$$MOI_{cylinder} = \begin{bmatrix} \frac{mass}{12} * (3 * radius^2 + height^2) & 0 & 0 \\ 0 & \frac{mass}{12} * (3 * radius^2 + height^2) & 0 \\ 0 & 0 & mass * \frac{radius^2}{2} \end{bmatrix} \quad (2)$$

To approximate the decay rate for the object, Satellite Tool Kit (STK) was used. A representative 'satellite' body was input into a simulation that matched the specifications from Table 1. Then a model was created using the specifications for the lifetime calculations in Table 2.

Table 2: STK Model Specifications

Mu	3.99E+14 m^3s^{-2}
atmospheric density model	MSIS 1986
C_D	2.2
C_r	1
Drag area	29 m^2
Area exposed to sun	77 m^2
Solar flux sigma level	0
Solar flux file	solflx_schatten.dat
Argument of Perigee	0 rad
RAAN	0 rad
True Anomaly	0 rad
Orbit Epoch	2 Aug 2016 16:00:00.000 UTCG

The STK orbital model was run for a rocket body starting at 1100 km altitude and decreasing the altitude by 100 km each time. The inclinations considered were 89 and 92 degrees due to the high interest in the number of objects in these orbits, 53 degrees chosen for the

approximate inclination of the International Space Station (ISS), 23 degrees chosen for the launch inclination of Cape Canaveral, Florida and 0 degrees as a control case [2].

The Delta-V required by a single rocket to change its orbit from the above parameters to bring it down to a 300 to 600 km orbit in 100 km increments from starting altitudes of 400 to 1100 km orbits was calculated. If drag alone is not sufficient to deorbit a rocket in the required 25 year time limit, an additional propulsion source will be required.

For a chaser and target case (i.e. the "combined case"), to determine the impact of a stable joint configuration with two rocket bodies joined by a tether as shown in Figure 12, the set of parameters in Table 3 was used, and the STK model run using the same parameters listed in Table 2 using the method in the previous paragraph.

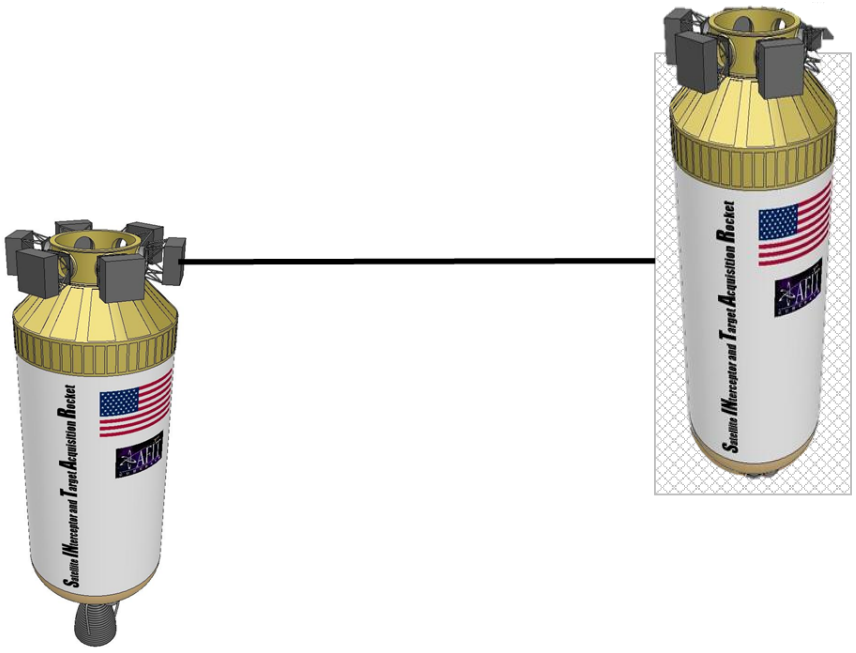

Figure 12: Combined Rocket Configuration after impact of net but before release of a drag chute or firing of additional propulsion systems for deorbit

This configuration was chosen based on the desired target, a dead rocket body, rather than the modeled mission concept seen later in this section. To determine the combined MOI of the system the Parallel Axis Theorem was used as shown below.

$$I_{combined} = I_{catcher} + I_{target} + md^2 \quad (3)$$

Eq. (3) is only valid for a rigid body and would not work on a non-rigid body problem. To account for this in the presented research it has to be assumed that the tether is taut when this equation is applied. For future research adapting Eq. (3) to a flexible system may be preferable.

Table 3: Combined 2 Rocket Body System with Tether and Net

Weight (including net)	4541 kg		
MOI (in thousands) (kg*m^2)	23100	0	0
	0	23100	0
	0	0	23050
Drag Area (assume both rockets head on)	58 m^2		
Area Exposed to Sun (assume both rockets side on)	155 m^2		

Finally, a case was created using only the 89 degree inclination circular orbit between 700 and 1100 km to determine the benefits gained by additional drag as if a drag altering device had been deployed. The 89 degree orbit was chosen based on it being one of the two orbits of interest. These were compared using a multiplication factor to the drag area of the combined system using the numbers from Table 3 as a control case. All data was compared with a percent change to their respective controls for each data point comparison as well as an average across all altitudes.

Chaser, Target, Net and Drag Chute Modeling

The model simulation was developed to observe the dynamics of the system from the point of a stable chaser until the deployment of the drag chute. It was assumed that the chaser would remain fixed linearly at the origin of the simulation, however it would be allowed to rotate due to reaction forces from deploying objects. The initial phase as seen in Figure 13, was established as a steady state to better be able to observe reactions.

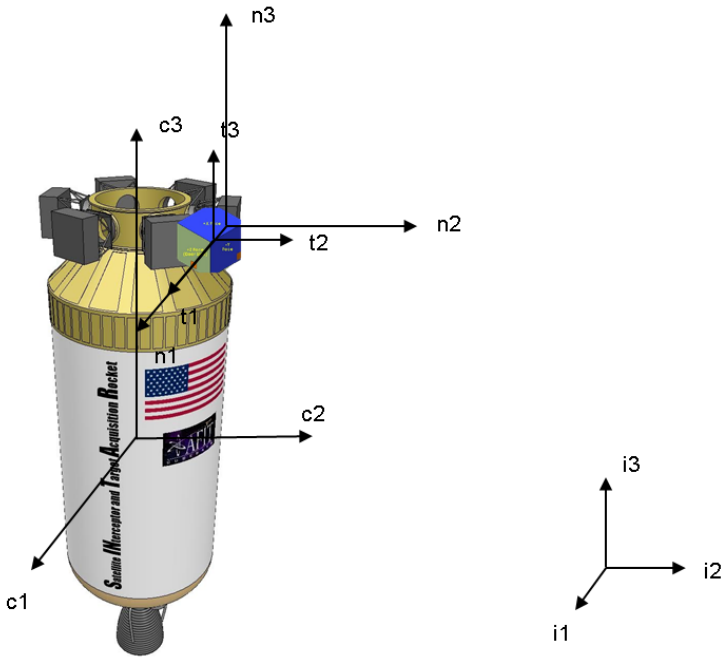

Figure 13: Phase 1 – Initial Steady State of System. The 'i' frame refers to the inertial. The 'c' frame refers to the chaser. The 't' frame refers to the target. The 'n' frame refers to the net. Not pictured is the drag chute frame which would be labeled as 'd'

Other necessary assumptions included initial conditions and attributes of the different objects modeled as listed in Table 4. The main objects accounted for include the chaser, target, net, each bullet, drag chute and tether.

Table 4: Object attribute initial conditions and source

Object	Element Definition	Initial Condition	Units	Assumptions/Source
Chaser	Mass	2247	kg	No fuel, single engine from NASA internet information page [35]
	Radius	3.05	m	from NASA internet information page [35]
	Height	12.67	m	Not including ESPA ring, from NASA internet information page [35]
Target	Mass	54	kg	Max weight of 27U [36]

	Depth (x)	0.3328	m	Max dimensions of 27U [36]
	Width (y)	0.3525	m	Max dimensions of 27U [36]
	Length (z)	0.366	m	Max dimensions of 27U [36]
	Speed	1	m/s	Anticipated speed based on CSD user guide [36]
Net	Mass	0.33	kg	Based on previous research [23]
	Length	24	m	Based on previous research [23]
	Height	24	m	Based on previous research [23]
	Width	0.01	m	Based on previous research [23]
	Speed	*speed_bullet* *cos(*bullet_angle*)	m/s	Anticipated speed based on geometry in the x-direction
	Stowed length	0.1	m	Initial condition until deployed for MOI contribution purposes, dimensions of 1U [29]
	Stowed height	0.1	m	Initial condition until deployed for MOI contribution purposes, dimensions of a 1U [29]
	Stowed width	0.1	m	Initial condition until deployed for MOI contribution purposes, dimensions of a 1U [29]
Bullet (x4)	Mass	0.5	kg	Based on previous research [23]
	Deployment angle	8	deg	Based on previous research [23] (see Figure 16)
	Speed	3	m/s	Upon deployment [23]
Net Electronics	Mass	21.3	kg	Based on previous research [23]
Tether	Length	100	m	Based on previous research, Max length, Negligible mass [23]
Drag Chute	Mass	0.28	kg	Assuming Mylar material weight 0.7 g/m^2
	Length	20	m	Assumes 400 m^2 chute
	Height	20	m	Assumes 400 m^2 chute

	Width (thickness)	4.5E-6	m	Based on NASA proposed Solar Sail mission [37]
	Stowed length	0.1	m	Initial condition until deployed for MOI contribution purposes, dimensions of a 1U [29]
	Stowed height	0.1	m	Initial condition until deployed for MOI contribution purposes, dimensions of a 1U [29]
	Stowed width	0.1	m	Initial condition until deployed for MOI contribution purposes, dimensions of a 1U [29]

The governing equations of motion are second order ordinary differential equations (ODE) and they are implemented in the simulation using a non-stiff medium order method known as ODE45 [38]. ODE45 is based upon the Dormand-Prince pair which is an explicit Runge-Kutta formula [38]. In order to model the system, state space equations are being used as seen in Eqs (4) and (5) which show the state derivative of a linear system.

$$\dot{\bar{x}} = \mathrm{A}\bar{x} + \mathrm{B}\bar{u} \tag{4}$$

$$\bar{y} = \mathrm{C}\bar{x} + \mathrm{D}\bar{u} \tag{5}$$

Where $\bar{x}$ (t) is an *n*x1 vector known as the state vector which can be a function of time. A is the state matrix, B is the input matrix, and $\bar{u}$ is the input and can be a function of time. C is the output matrix, D is the direct transition of feedthrough matrix and $\bar{y}$ is the output of the system. For this scenario there is no D matrix because the system does not have any feedthrough components. The input used is the quaternions, angular rate, linear position and linear velocity of each object. The total state vector is 114 elements long however when evaluated it is broken up into 13 element chunks. The output is the updated initial state at every time step.

Required for the ODEs using the state space equations are a system state vector and time vector. The state vector $\bar{x}$ is 13x1 for each of the represented objects. There is a separate state vector for each of the following, chaser, target, net, drag chute and each of the four bullets. As a result of these vectors A is 13x13, B is 13x1, C is 1x13, as seen in Eqs. (6)-(8), and D is 0 and thus not shown below. The zero elements within the matrices represent elements that do not have any cross coupling in the states.

$$A = \begin{bmatrix} 0 & 0 & 0 & 0 & 0.5*q4 & -0.5*q3 & 0.5*q2 & 0 & 0 & 0 & 0 & 0 & 0 \\ 0 & 0 & 0 & 0 & 0.5*q3 & 0.5*q4 & -0.5*q1 & 0 & 0 & 0 & 0 & 0 & 0 \\ 0 & 0 & 0 & 0 & -0.5*q2 & 0.5*q1 & 0.5*q4 & 0 & 0 & 0 & 0 & 0 & 0 \\ 0 & 0 & 0 & 0 & -0.5*q1 & -0.5*q2 & -0.5*q3 & 0 & 0 & 0 & 0 & 0 & 0 \\ 0 & 0 & 0 & 0 & 0 & -(I22*w3)I11 & (I33*w2)/I11 & 0 & 0 & 0 & 0 & 0 & 0 \\ 0 & 0 & 0 & 0 & (I11*w3)/I22 & 0 & -(I33*w1)I22 & 0 & 0 & 0 & 0 & 0 & 0 \\ 0 & 0 & 0 & 0 & -(I11*w2)/I33 & (I22*w1)/I33 & 0 & 0 & 0 & 0 & 0 & 0 & 0 \\ 0 & 0 & 0 & 0 & 0 & 0 & 0 & 0 & 0 & 0 & 0 & 0 & 0 \\ 0 & 0 & 0 & 0 & 0 & 0 & 0 & 0 & 0 & 0 & 0 & 0 & 0 \\ 0 & 0 & 0 & 0 & 0 & 0 & 0 & 0 & 0 & 0 & 0 & 0 & 0 \\ 0 & 0 & 0 & 0 & 0 & 0 & 0 & 0 & 0 & 0 & 0 & 0 & 0 \\ 0 & 0 & 0 & 0 & 0 & 0 & 0 & 0 & 0 & 0 & 0 & 0 & 0 \\ 0 & 0 & 0 & 0 & 0 & 0 & 0 & 0 & 0 & 0 & 0 & 0 & 0 \end{bmatrix} \quad (6)$$

$$B = \begin{bmatrix} 0 \\ 0 \\ 0 \\ 0 \\ (R\_bi11*(T1))/I11 + (R\_bi12*(T2))/I11 + (R\_bi13*(T3))/I11 \\ (R\_bi21*(T1))/I22 + (R\_bi21*(T2))/I22 + (R\_bi23*(T3))/I22 \\ (R\_bi31*(T1))/I33 + (R\_bi32*(T2))/I33 + (R\_bi33*(T3))/I33 \\ 0 \\ 0 \\ 0 \\ 0 \\ 0 \\ 0 \end{bmatrix} \quad (7)$$

$$C = [1\ 1\ 1\ 1\ 1\ 1\ 1\ 1\ 1\ 1\ 1\ 1\ 1] \quad (8)$$

At every time-step, a check of both angular and linear momentum is conducted to ensure the law of conservation of momentum is not violated. The equations for linear and angular momentum are seen in Eqs. (9) and (10) respectively, where *m* is the mass and **I** is the MOI of the objects.

$$\bar{p} = m\bar{v} \tag{9}$$

$$\bar{L} = \mathbf{I}\bar{\omega} \tag{10}$$

The principle MOI's needed to conduct the calculations in the simulation are approximations based on the shape of the objects. Two different shapes were used to make these approximations, box and cylinder. The chaser and the bullets use the cylinder approximation shown in Eq. (2) and the net, drag chute, and target are approximated as a box as shown in Eq. (11).

$$\mathrm{MOI}_{\mathrm{box}} = \begin{bmatrix} \frac{\mathrm{mass}}{12} * (\mathrm{width}^2 + \mathrm{depth}^2) & 0 & 0 \\ 0 & \frac{\mathrm{mass}}{12} * (\mathrm{depth}^2 + \mathrm{height}^2) & 0 \\ 0 & 0 & \frac{\mathrm{mass}}{12} * (\mathrm{width}^2 + \mathrm{height}^2) \end{bmatrix} \tag{11}$$

At the initial state, all components are stationary with respect to each other. During the second phase, a target is released by way of a CubeSat deployer, such as PSC's CSD, as seen in Figure 14.

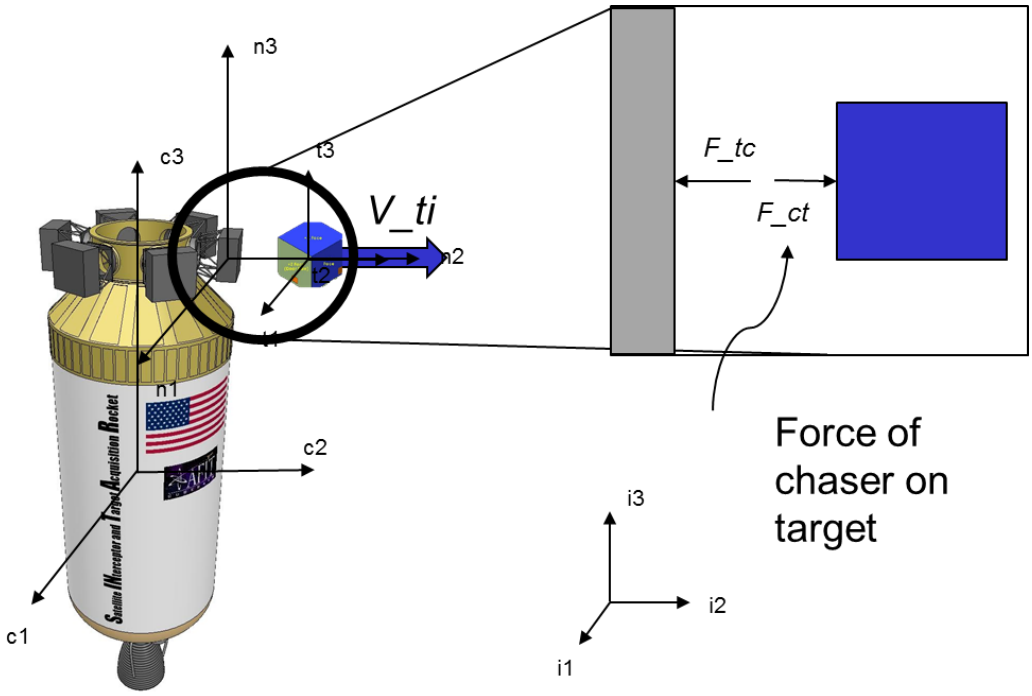

Figure 14: Phase 2 – Deployment of the target

The second phase only lasts as long as the force is applied to the target. The force is centered on the plate of the target closest to the center of the chaser for approximately 0.1 s. The resultant torque caused by the target pushing on the chaser during the deployment is calculated using Eq. (12) while an approximation of the acceleration is calculated from the expected duration of the force being applied and the final velocity as seen in Eq. (13). There is no torque on the target caused by the chaser pushing back due to the force being applied through the origin, assumed center of mass, along an axis. The tether is not considered in the system yet since it is only exerting a force when in tension.

$$g = distance * force \tag{12}$$

$$acceleration = velocity/time \tag{13}$$

After the target has been successfully deployed and is only at a constant velocity after being ejected from the CubeSat deployer, the scenario enters Phase 3 as seen in Figure 15.

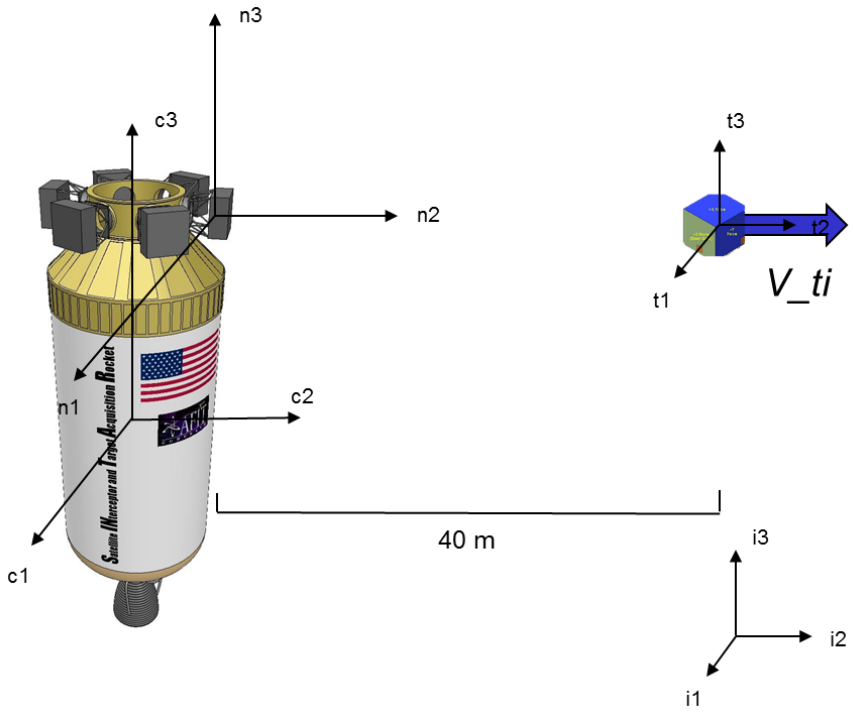

Figure 15: Phase 3 – Target drifts away from chaser at approximately 1 m/s

Net Deployment and Target Capture

Once the target has reached a pre-arranged distance from the chaser, a net will be deployed. The distance can be adjusted based on the length of the tether, velocity of the target and expected velocity of the net. For this simulation, it was considered to be a constraint that the net would deploy once the target reached a distance of 40 m. This would allow the net to be almost fully extended by the time it was expected to impact the target at an expected distance of 60 m. The net deployment consists of four bullets shot simultaneously from the canister towards the target. The bullets each weigh approximately 0.5 kg and are propelled at a rate of 3 m/s at an angle of 8 deg off the centerline as seen in Figure 16 and Figure 17 of Phase 4.

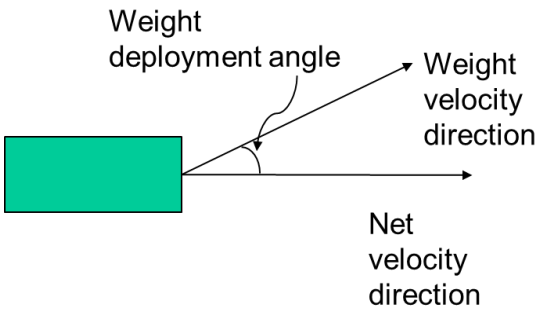

Figure 16: Bullet deployment angle

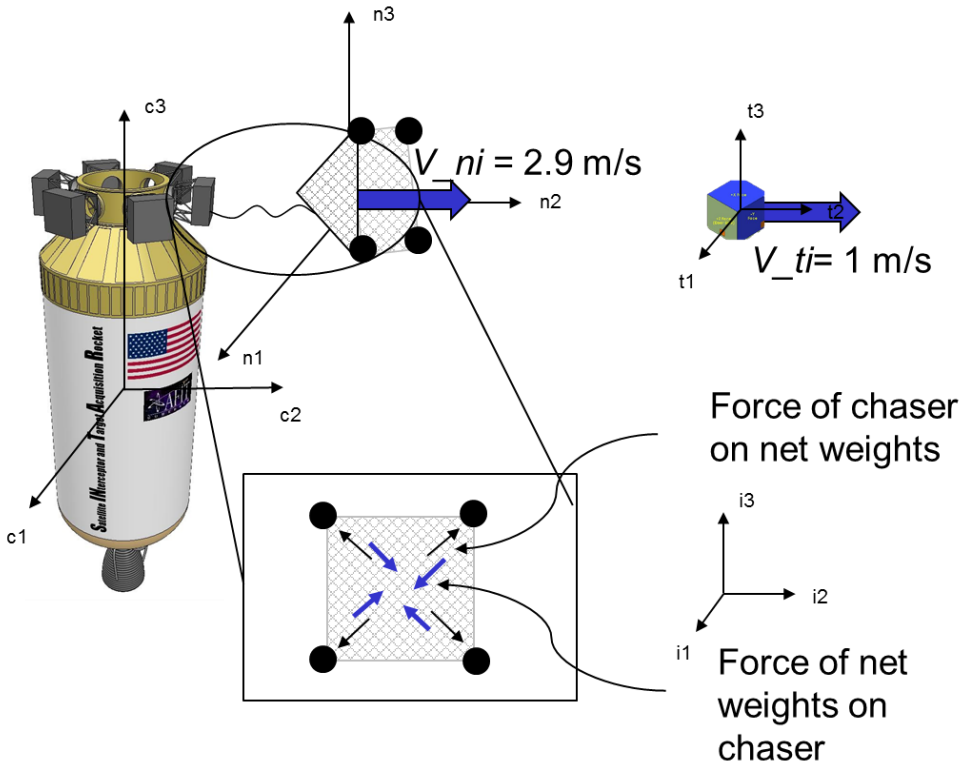

Figure 17: Phase 4 to 7 – Deployment of bullets and net. The bullets accelerate and then drift until they pull the net vertex out which accelerates and then the combined system drifts towards the target

The subsequent stages include the capture of the net and the pulling of the tether taut before the release of the drag chute as seen in Figure 18 and Figure 19.

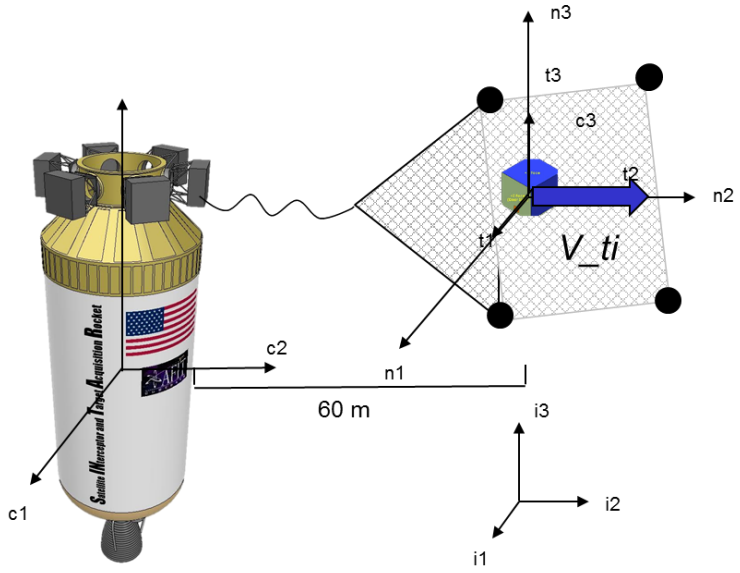

Figure 18: Phase 8 – Net captures the target decelerating the net and accelerating the target

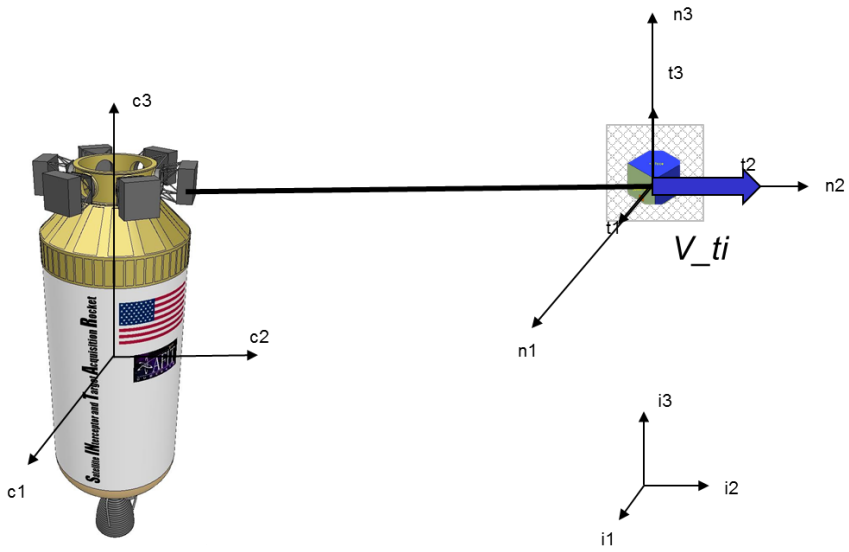

Figure 19: Phase 9 – The combined net and target drift until they reach the length of the tether, 100 m

The velocity of the combined systems was calculated via the principle of conservation of momentum. Using Eqs. (9) and (10), the momentum of each object was calculated and then

combined for the total momentum of the system. The resulting velocity of the combined system must have the same momentum so the total momentum was divided by the total mass of all the objects after impact assuming no losses. After the tether reached a length of 100 m, then the drag chute was deployed as seen in Figure 20 and Figure 21.

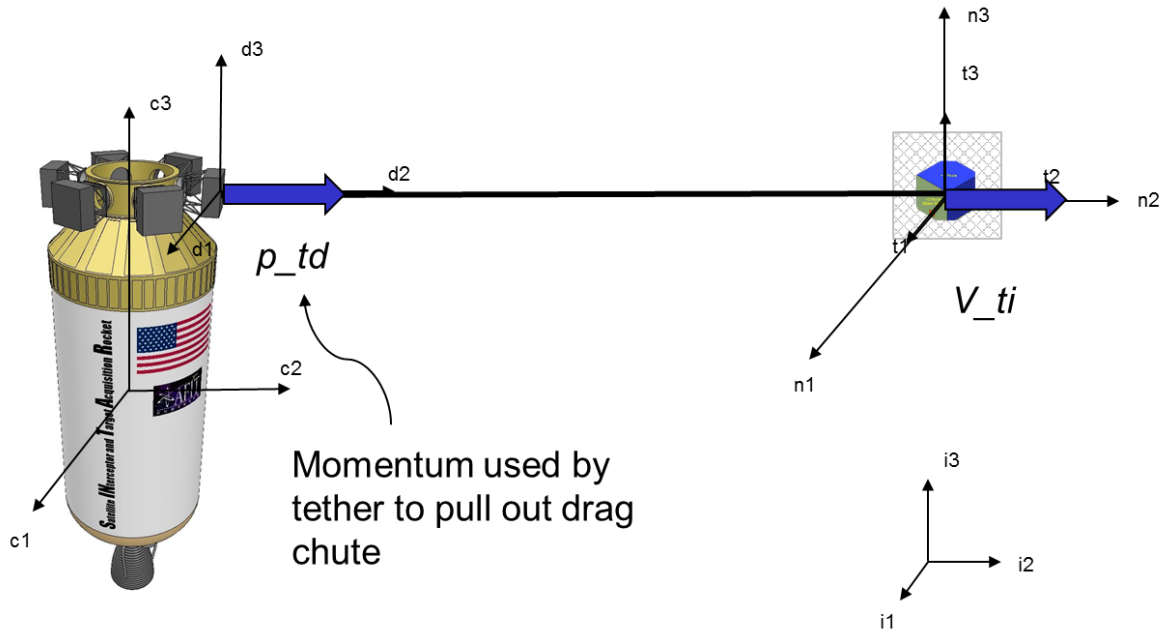

Figure 20: Phase 10 – Release of drag chute from chaser

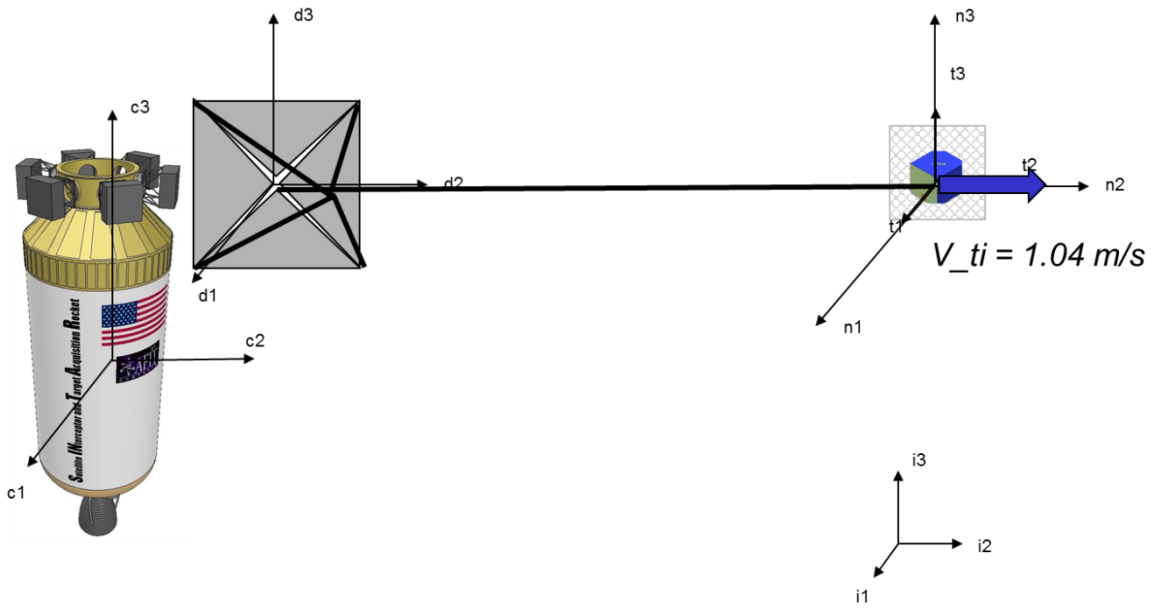

Figure 21: Phase 11 - Deployment of drag chute. Phase 12 (not pictured) – Deorbit of target

The force exerted by the drag chute is dependent upon initial conditions including the size of the chute, orbital altitude and weight of objects attached to the chute. The orbital velocity was determined using Eq. (14) where $M_{central}$ is the mass of the earth, G is the gravitational constant and R_E is the radius from the center of the earth to the satellite.

$$v = \sqrt{\left(\frac{G * M_{central}}{R_E}\right)} \tag{14}$$

The density is determined based on the current altitude of the drag chute at the time of the calculation. For the purposes of this research, the altitude was considered to be constant, so the simulation would not take the target all the way to burnup, rather, the simulation would end soon after the drag chute deployment. A more detailed simulation could be run for future work to model all the way through burnup of the target. Eq. (15) provides a relatively simple relationship between density and altitude which is determined with the scale height being found in a lookup

table and where ρ_o is the density at a reference altitude [39]. The equation is a very simplified assumption.

$$\rho = \rho_o * e^{-\frac{altitude}{scale\ height}} \tag{15}$$

The coefficient of drag C_d for a satellite in orbit that is not a sphere is generally assumed to be 2, which was used in this simulation [39], thus the resulting force of the chute is calculated using Eq (16). The force calculated was then transformed into an acceleration using Newton's Second Law as seen in Eq. (17)

$$F = \frac{1}{2} * \rho * \frac{A_{chute}}{m} * C_d * v^2 \tag{16}$$

$$a=F/m \tag{17}$$

System Deorbit

The design of the deorbit required careful thought to attempt to eliminate or reduce the issue of potentially crashing the target or chaser into the other. The approach of using the main engine on the chaser was evaluated but removed as potential solution because it was determined that resultant orientation of the chaser and target after firing the engine would put the target directly behind the chaser in line with the chaser engine. This orientation would result most likely in break in the tether or a collision between the target and chaser. The chaser engine and any remaining fuel is only used to deorbit the chaser. The primary deorbit method evaluated for the target was a drag chute deployed from the ESPA ring at the opposite end of the tether from the net as shown in Figure 21. First, the chaser would move out of range of the target and drag chute doing its deorbit burn, and then the drag chute could be fully extended. The estimated time for the drag chute to fully extend is 3 s in the simulation. The speed at which it is deployed is not dependent on the need for the force provided by the drag chute to prevent windup of the target

and tether. To accomplish this arrangement the drag chute would be encased in another small CubeSat, either 1U or 2U in size, which will deploy independently after a given condition. The specifics on how it deploys was considered to be future work.

The drag method was evaluated to determine if a reasonable size chute would work at the desired altitudes using STK as described in the Target Orbital Life section below. The force from chute size determined from the STK model was then applied to the model to observe the dynamics of the system. If the drag chute method did not work, an electric motor propulsion method would be needed. An electric motor propulsion method was not evaluated in the demonstration mission concept model; however, cases where it would be required were noted. The requirement is to deorbit the rocket to the point that it would decay within at least 25 years as a threshold value, however, the objective value would be within 1 year.

Summary

In this chapter, the methodology of the simulations was covered. This included how the STK models were established for orbital lifetime calculations. Also discussed were the important equations needed to model the system during the capture to observe the dynamics. The results and analysis of these calculations are discussed in the next chapter.

IV. Results and Analysis

Chapter Overview

In this chapter, the results of the calculations and models will be discussed. An analysis was performed on the results of the STK modeling to quantify the impact of the proposed mission. Analysis was also conducted on the dynamics model to determine constraints of the proposed system. Specific areas that were analyzed in the simulation include the effects of the net not hitting the target in the center of the net, impacts of a tip-off angle change to one of the bullets upon firing, a mis-firing of one bullet which changes its speed and a varying of the deployment speed of the target.

Results

Target Orbital Life

The first set of data obtained from the model results generated using STK was the lifetime of a Single Engine Centaur that was varied over a circular orbit in different inclinations and altitudes. Altitudes were chosen based on research showing a current level of high density such as at 89 and 92 degrees, high interest orbits due to use such as the ISS and Cape Canaveral and 0 degrees to be used as a control. The results of these initial runs are shown below in Fig. 22.

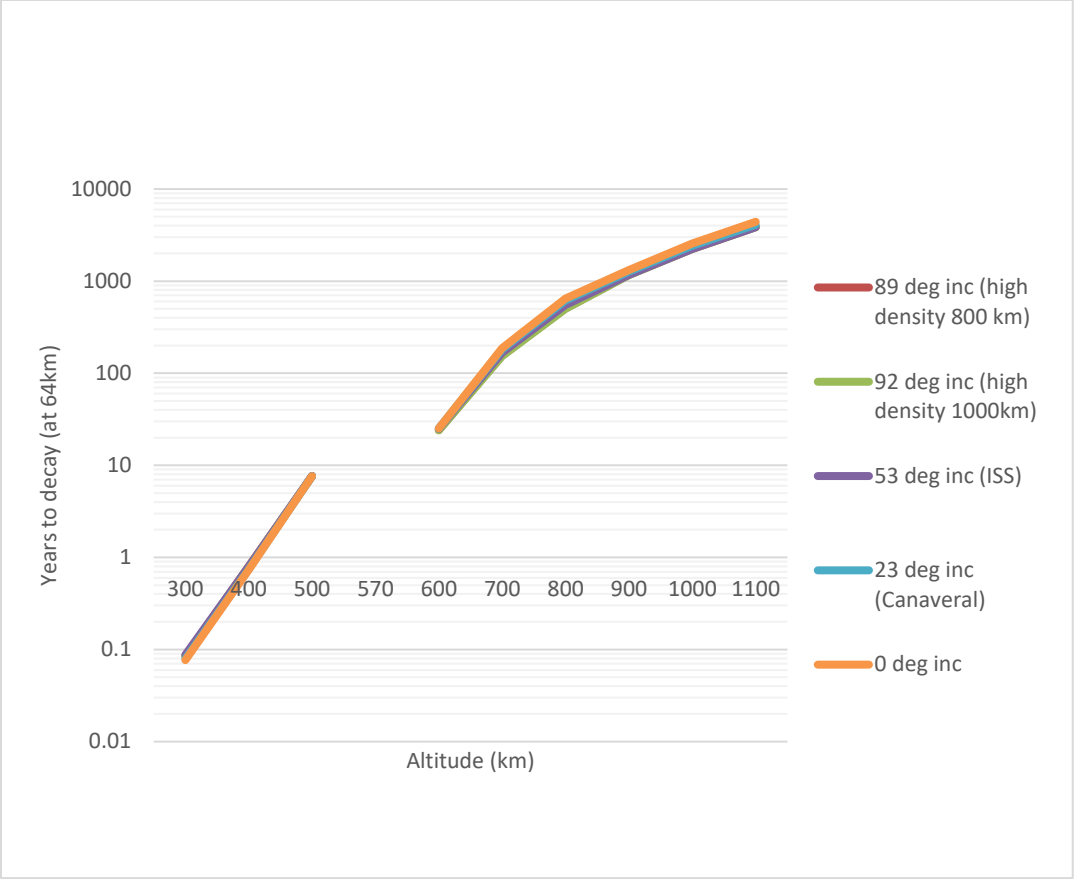

Figure 22: Lifetime of Empty Single Engine Centaur Rocket Body. No data point is shown at 570 km however is later used as a point of interest being the 25 year break point

The results of this analysis showed that there is not much difference in the time for a satellite to decay based on altitude below 600 km. Past 600 km orbits, however, the range also goes beyond the 25 year requirement to deorbit. The high-density orbit of 89 degrees at 800 km would deorbit within approximately 500 years while the 92 degree orbit at 1000 km would take approximately 2200 years.

When the chaser and target which was similar size to the chaser were modeled as one combined system (connected by a tether), to be referred to as the dual rocket system or dual system, similar results were discovered as shown in Figure 23. The 89 degree at 800 km orbit

was now 510 years, a 0.84 percent increase over the single rocket system, and the 92 degree orbit at 1000 km was now 2258 years, a 1.04 percent increase. All of these are within the error of the model and could be considered to have no change.

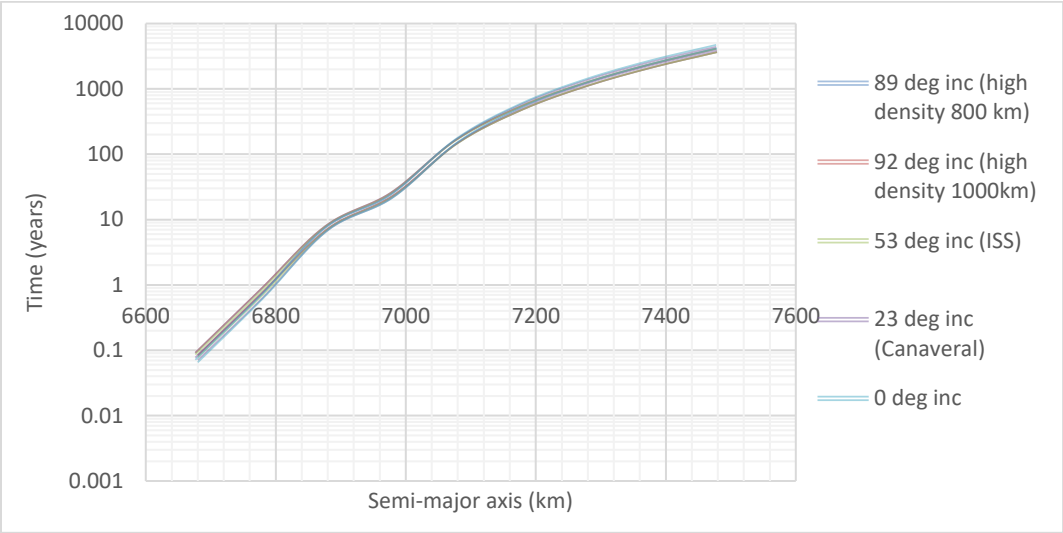

Figure 23: Dual Rocket Body Deorbit Times

The percent increase showed similar results for all of the different orbits at each altitude. The one exception was 53 degree and 0 degree inclinations at 300 km orbits which did not have any change where the others had about 3.5% increase as seen in Figure 24. All of the orbits averaged about a 1% increase in total time to deorbit in the dual configuration over the single rocket body configuration. The percentage seen was within the error of the system.

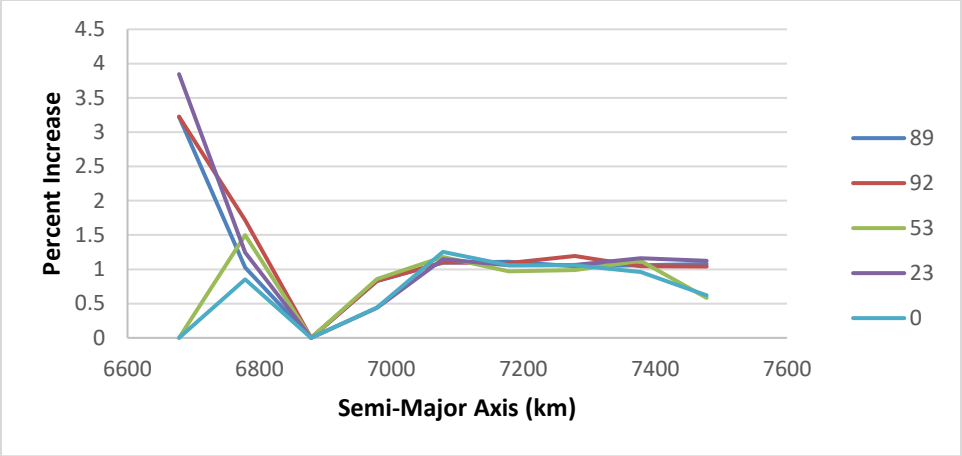

Figure 24: Percent Increase from Single Rocket to Dual Rocket System (Without Added Measures)

The observed decay time at the orbits of interest poses a problem if an additional deorbit method is not also employed. When looking at methods and ways to implement an additional deorbit method two main ideas are typically used, a deorbit burn or drag. A majority of the time is spent at the higher altitudes and until they reach a certain height, the effects of drag are not reducing the overall orbital lifetime. This overcomes the time spent in the lower altitudes where the drag is affecting the altitude. When a spacecraft or debris starts lower, already in the drag environment, or so close that minimal time is spent outside of it, the decrease in altitude is seen more rapidly because of the increased drag. When an example case report was pulled from STK showing the orbital parameters over the course of the orbital lifetime as seen below in Figure 25 you can see a verification of this theory.

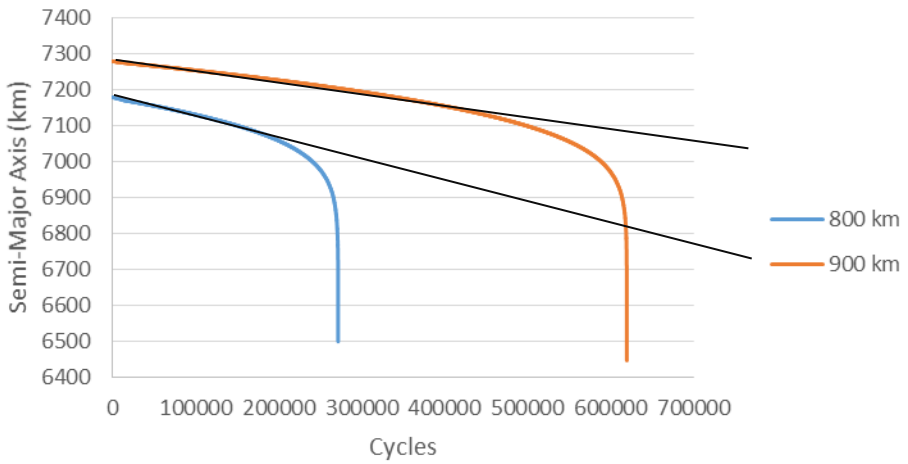

Figure 25: Comparison of 800 and 900 km orbits at 53 degree inclinations. Compares altitude each cycle. Black line indicates slope of initial part of curves

When a 900 km orbit at 53 degrees is compared with an 800 km orbit at 53 degrees it is seen that the early portion of the curve's slope is greater for the 800 km orbit. Ideally, if an additional source could speed up the process of getting to bend at 6950 km for the 900 km orbit the lifetime could be drastically reduced. As seen below in Table 6, if a maneuver were conducted in either orbit to reduce it to a 600 km orbit at the beginning of its life, the new lifetime would be 40 years. While this number is still above the required 25 years it significantly reduces the total time in orbit.

Table 5: Comparison of Orbital life for 53 degree inclination orbit at 800 and 900 km altitudes with and without maneuver to decrease orbit to 600 km at beginning of life

orbit (km)	start date	date at 6978.14 km	date of decay	old life (years)	new life (years)	difference (years)
800	8/5/2016	10/5/2487	11/1/2527	51	40.1	471
900	8/5/2016	5/28/3160	8/6/3200	1184	40.2	1144

For an 800 km orbit, this is a 92% decrease in the orbital life and for the 900 km orbit a 96%. To achieve the desired 25 years, the orbit would need to be reduced to a semi-major axis of 6948.14 km or a 570 km altitude.

When looking at deploying only a drag chute as an augmented deorbit method for the combined system the results showed an almost exponential decay in total lifetime. This was more dramatic for the higher altitudes where the starting lifetime was higher than the lower orbits as shown below in Figure 26.

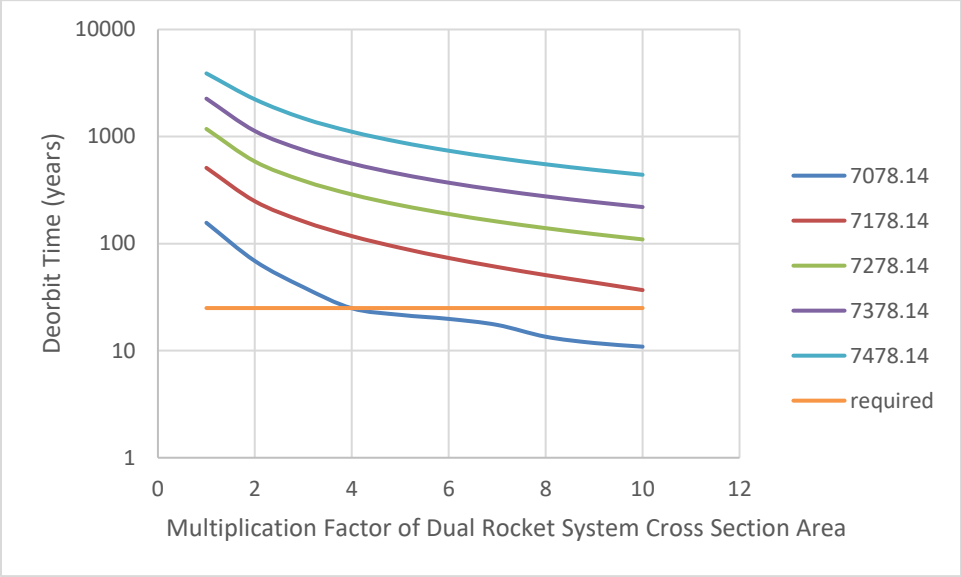

Figure 26: Change in Deorbit Time at 89 Degrees with Increasing Drag (Multiplication Factor of Dual System Cross Section Area)

Seeing the results of Figure 26, an analysis was conducted on the two target orbits of 89 degrees, 800 km and 92 degrees, 1000 km to determine how big a drag chute would have to be if used on just one rocket. As seen in Figure 27 below, an area of ~350 square meters is required for the 89 degree orbit, however, nearly 1850 square meters is required for the 92 degree orbit.

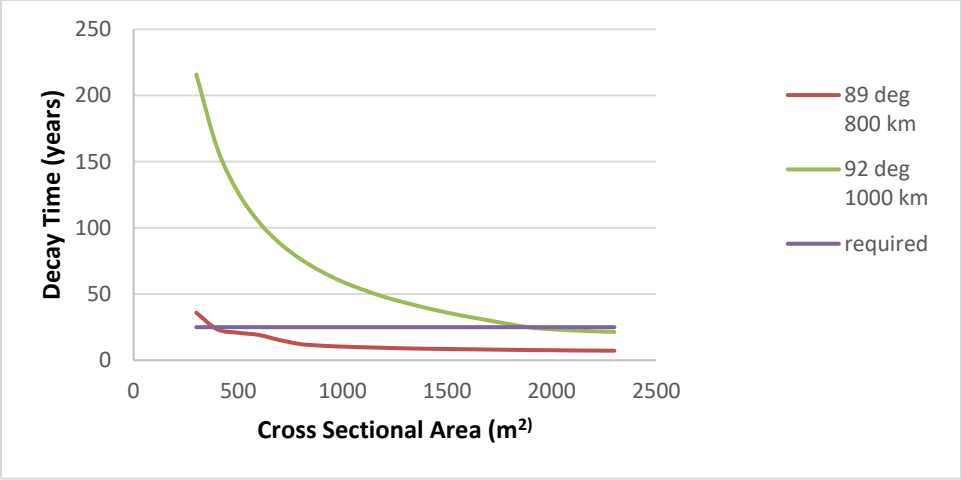

Figure 27: Required drag area for target orbits versus time to deorbit

Of note about the data was the appearance of a diminishing return line with increasing area. For the 89 degree orbit this line appeared around 7 years and for the 92 degree orbit this line appeared around 21 years. This shows that the best possible lifetime with a drag chute in these orbits is approaching 7 and 21 years, respectively. These achieve the desired threshold value of less than 25 years however for the 92 degree orbit the required area may be problematic. To achieve the objective value of less than a year and to not have an excessively sized drag chute an alternative would be required.

The final portion that was examined for this part of the study was the required delta-V to change the orbits. This did not take into account the different inclinations or starting and stopping a maneuver at a specific location in the orbit. In Table 6 below, there is a comparison from all orbit altitudes down to either 300, 400, 500 or 600 km orbits.

Table 6: Delta-V Required to Change from One Orbit to Another for a Single Centaur

Initial Orbit Altitude (km)	Delta V to 300 km (m/s)	400 km (m/s)	500 km (m/s)	600 km (m/s)
300	0	0	0	0
400	28	0	0	0
500	56	28	0	0
600	84	55	27	0
700	111	82	54	26
800	138	109	80	53
900	164	135	106	79
1000	190	160	132	104
1100	215	186	157	129

After noticing the stark change in the orbital lifetime curves in Figure 25, it would make sense that all that is required would be to decrease the orbit to at least the 600 km altitude or 6978 km semi-major axis. The lower altitude will then cause the more rapid decay of the orbit. To conduct the maneuver discussed previously of getting to the 570 km altitude orbit the amount of delta-V required for the 800 km orbit would be 61 m/s and for a 1000 km orbit, 113 m/s. This is a 13% and 7% increase respectively over the amount needed to achieve the 600 km altitude orbit. However, this is a 55% and 40% decrease respectively over the amount needed to achieve the 300 km altitude orbit.

Further investigation was conducted to study the effects of the drag model chosen on the orbit lifetime and the valid range. The model used for the initial data set was MSIS 1986, which is an empirical density model based on satellite data and is valid from 90-1000 km [40]. A newer version was created in 1990, and this model is valid from 0-1000 km [40]. Because the model is not valid for 1100 km, this data is extrapolated and may not be as accurate as other models that have a higher range. The newest version of the model was created by the US Naval Research Laboratory in 2000, which also changed the way a certain routine was called in the code [40]. The only models that are valid past the 1000 km point are the Jacchia models, however, they are

older and do not use the recent satellite density mapping data [40]. A test was run to see the differences using the 23 degree 700 km orbit using both the dual and single rocket systems to also compare the percent improvements. As seen in Table 7, all models showed about a 1% worsening of the orbital lifetime from the single to the dual rocket system.

Table 7: Comparison of STK density models

Model	dual	Single	Improvement
MSIS 1986	158.4	156.6	-1.14%
MSISE 1990	154.8	153.1	-1.11%
NRLMSISE 2000	149.5	147.7	-1.21%
CIRA 1972	138.1	136.4	-1.24%
Jacchia-Roberts	136	134.4	-1.19%
Jacchia 1971	137.6	136	-1.17%
Jacchia 1970	151.1	149.3	-1.20%
Jacchia 1970 Lifetime	140.2	138.5	-1.22%
Harris-Priester	127.9	126.4	-1.18%
1976 Standard	50.7	50.2	-0.99%

The models developed by Hedin, such as MSIS and its updates, all range within a ten year time span for the results [40], the largest duration being the chosen model. This would make it the most pessimistic approach and a good start for a rough approximation. The 1976 Standard was a table look-up method that resulted in the shortest lifetime of only 50 years, even though the model was valid from 86 to 1000 km [40].

System Model

Modeling they dynamics of the proposed deployment-capture experiment system consisted of twelve different phases. The initial concept was modeled and the model predictions showed that when the target and net were deployed from the chaser a rotation was induced in the chaser as seen in Figure 28. The chaser showed a constant change following the deployment of

the target and an additional change following the deployment of the bullets and the net. All of the others remained constant at their initial attitude of [0 0 0 1] though out as expected due to several assumptions imposed upon the simulation and the graphs of their quaternions are not shown here. The vertical lines reflect the end of each phase.

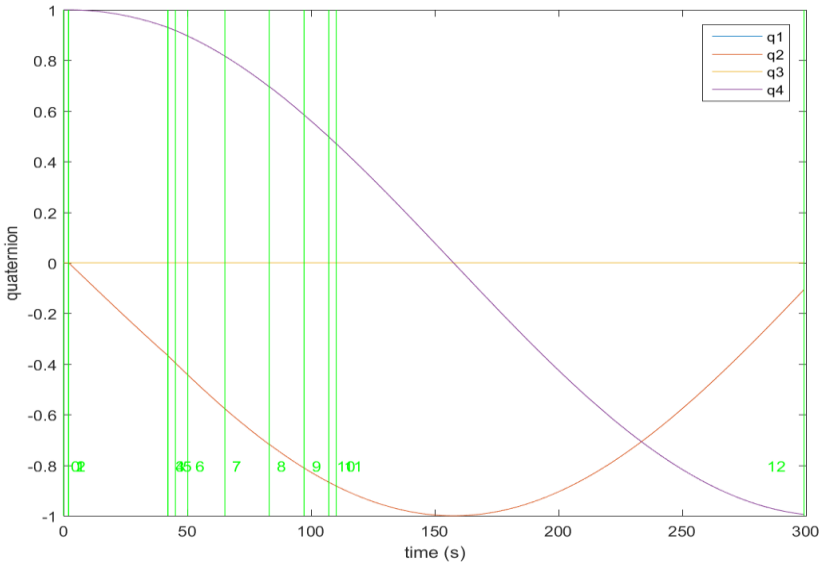

Figure 28: Quaternions of the Chaser (only q2 and q4 are changing)

The rotation of the chaser had an angular rate of 0.0187 rad/s after the target deployment and 0.0208 rad/s after the bullets are deployed. The torque on the chaser that would be applied with the deployment of the drag chute was not considered in this model due to the initial assumption that the chute is released only by the tether going taut and does not actually pull on the chaser's structure. The effects of the torques on the chaser as well as the possibility of the tether going taught prior to the drag chute release, should be considered in future work where a more detailed model of the system and the release of the drag chute is explored. For the purposes of the rest of this research, the torques applied to the chaser were removed with the assumption of an ADCS being implemented capable of handling the induced angular rates. Future work

should consider adding in active feedback control in the model to help determine the time required to combat the torque and re-align with the target for net deployment. After the adjustment involving the removal of the chaser torque, it was shown that the deployment of the target, bullets, net and drag chute did not induce an angular rate on the chaser. Ideal conditions were assumed for the model.

The initial case had the net impact the target in the exact center of the net with all bullets equidistant and traveling at the same velocity. Due to this configuration, all of the forces of the bullets were able to cancel each other out and no induced angular rate was seen on the target. Other than the primary control case, listed below are the variations examined:

- Impact location on net of the target from - 10 m to 10 m in both the x and y direction 0.2 m increments. (83% of total net area) with [0, 0] being the control and the full size being 24 m by 24 m (area covered is 20 m by 20 m)
- Target deployment velocity varied from 0.5 to 2 m/s at 0.5 m/s increments with 1 m/s being the control
- One Bullet deployment angle varied between 5 and 10 degrees at 1 degree increments with 8 degrees being the control
- One Bullet velocity varied between 1 and 5 m/s at 0.5 m/s increments and 3 m/s being the control

These cases were chosen based on the greatest likelihood of mission impact and chance of occurrence from a chosen group of experts [41]. The nominal case was considered the control with the results shown in Table 8, which includes all parameters considered for comparison across the different scenarios.

Table 8: Control Run results of selected criteria comparing expected versus observed values

Criteria	Expected	Observed	Difference Cause
Target Deployment Velocity (*x*)	1 m/s	0.99 m/s	Time resolution of simulation
Net Vertex Velocity (*x*)	2.9 m/s	1.62 m/s	How the firing angle was initially calculated and implemented in the simulation
Target and Net Combined Velocity (*x*)	1.3 m/s	1.02 m/s	Difference in the net vertex velocity
Induced Angular Rate of Target After Net Impact	0 rad/s	0 rad/s	For ideal case, results as expected
Force of Drag Chute	Very High	0.0045 N	Did not accurately account for the continuous acceleration
Velocity Change by End of Scenario after Chute Deployment	Very High	-0.02 m/s	Difference in the force of the drag chute

Of note is the difference in the expected vs observed results for the deployment velocities, combined target, and net velocity and the force of the drag chute applied on the target. The target deployment velocity difference as shown in Table 8 is likely due to the time resolution of the simulation and the time step used in that phase. As future work, it was recommended to adjust the time step to get better resolution of this velocity. The net deployment velocity difference as shown in Table 8 is due to the way the deployment angle was calculated in the rough calculations and the final simulation. The final simulation is correct for the way it was desired to be implemented. The combined velocity difference as shown in Table 8 is due to the inaccuracy of the target deployment velocity and the drastically different net deployment velocity. The force of the drag chute as shown in Table 8 was expected to be a very large number

(1000+ N) due to the lifetime calculation done prior to the simulation. Based on the scenario parameters of 300 km it was expected that the combined target, net and drag chute system would deorbit in less than a day if the chute deploys to its full 20 m x 20 m size. If the chute failed to deploy, it was estimated that it would take the target and net system 6.1 years to deorbit. The difference in the expected and observed values in the drag chute force numbers as shown in Table 8 is due to the non-linear nature of the force over the course of the lifetime that in the 300 s of the scenario was treated as a constant acceleration and linear velocity change. The drag chute force is constantly being applied which allows for a continuous acceleration during the entire deorbit, which was not modeled. If the force had been applied, the position of the target would have an exponential altitude decay and would the less than 1 day lifetime results.

For the net location impact case a batch run was created. It accounted for every offset from – 10 to 10 m in y- and z- directions from the center point of the net every 0.2 m. For this case, it was assumed that the net was traveling directly at the target and it and the target's velocity vector directions matched (+x only). For future work, it is recommended to account for velocity vector directions that do not match. The scenario was only run up until the target and net were traveling as a combined system. The induced angular rate of the target was then estimated. The predictions were then compared against the expected angular rate the drag chute could overcome based on the control case's observed force. Figure 29 shows that most locations for impact induced an angular rate too large for the force of the net to overcome by itself. The figure shows in red any location on the net that if the target impacted there the drag chute would not be able to overcome the induced angular rate whereas the green highlights locations that can. Each position on the chart is a 0.2 by 0.2 m section of the sampled area and the values represent the

expected induced angular rate if the target were to impact that location. The top and right highlighted areas are believed to be artifacts of the simulation and not true impact points.

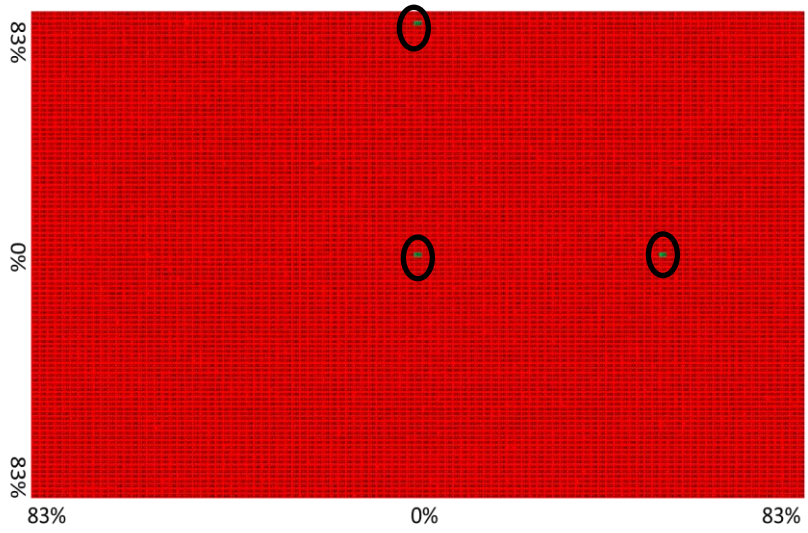

Figure 29: Impact locations capable of inducing an angular rate that can be overcome by the deployment of the drag chute. Center point is center of net. Percentages are based on the percentage of the radius covered from the center point

The outcome where very specific locations must be hit on the net by the target was determined to not be an acceptable scenario based on previously established mission parameters and desire for mission success. In an effort to determine if there was a simple mission design parameter that could be adjusted to account for this another calculation of the force was done as if the drag chute had to be released from the chaser 0.1 s after the tether goes taut. The new force was calculated to be 2292 N due to the resistance of the massive chaser with respect to target. The force of the drag chute is not considered in this number since the chute has not been released yet. The calculation made assumes that momentum is conserved and that the force is applied as a constant over the 0.1 s time. Using this new force and the same calculations from before Figure 30 shows that any impact point on the evaluated area is feasible for the target not to roll up into the drag chute.

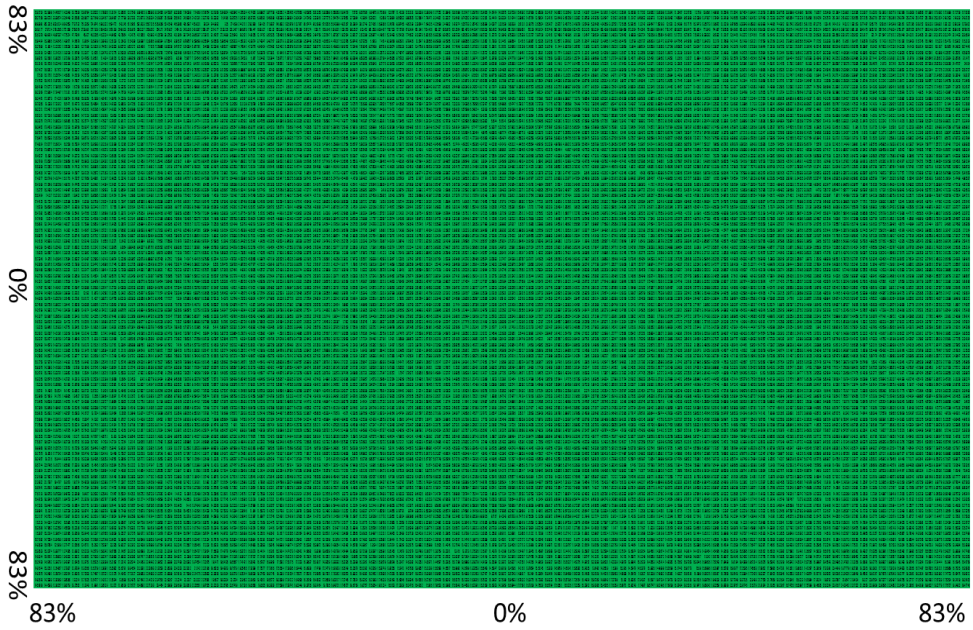

Figure 30: Feasible impact locations of target on net if tether is held taut by the chaser for 0.1 s before the drag chute is deployed

While these results are more promising, they do not account for any "yo-yo" oscillatory action of the target as it is decelerated from its spin caused by the deployment of the drag chute. For the higher initial rotational rates it is expected that if the deceleration is too sudden than the target will begin to rotate in the opposite direction after becoming fully extended. This "yo-yo" action was not modeled in this simulation however should be considered for future work to further investigate the feasibility of the presented concept. The action of the target rotating will cause the target to wind the tether around itself. It will continue to move in the x direction at 1.02 m/s however the tether will become taut much faster than its control case of 14 s post target and net impact. To account for this an analysis was done on which locations would cause the target to rotate and wind up the tether faster than 14 s. In Figure 31 it was shown that a radius of 80% would always wind up at a rate that would take longer than 14 s.

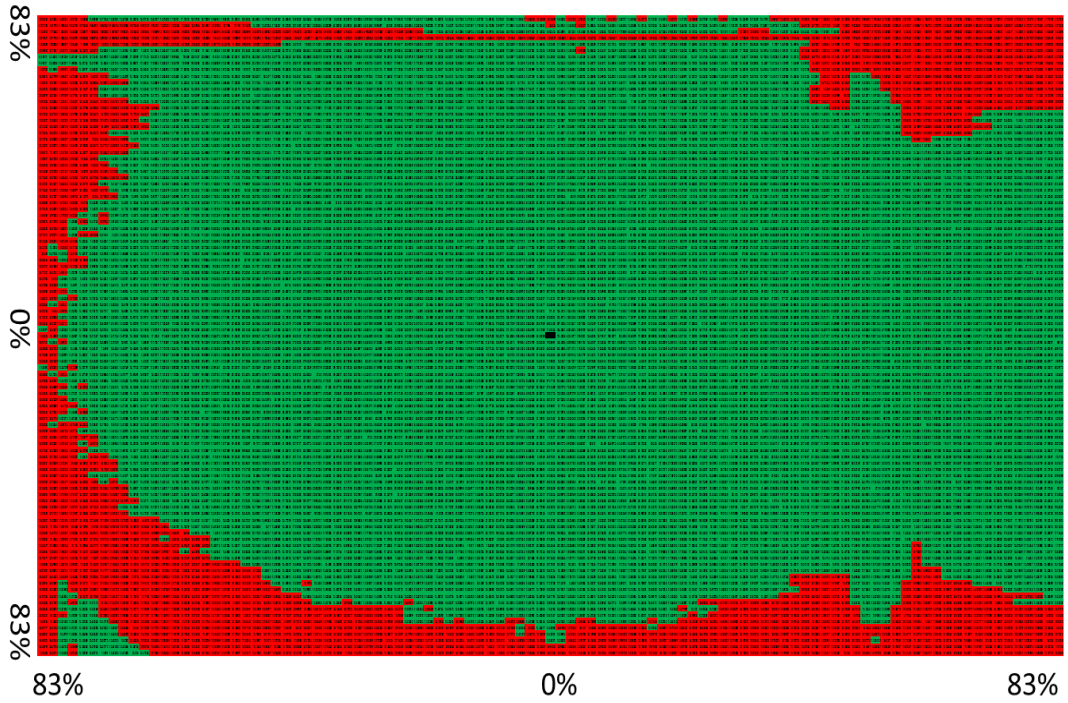

Figure 31: Impact locations that induce an angular rate that would take longer than 14 s to wind up the entire 100 m tether without accounting for target linear drift. The center is denoted with a black square

After the data was analyzed using these criteria it was determined that the time needed to be adjusted to account for the continued drift of the target as well. The updated results are seen in Figure 35.

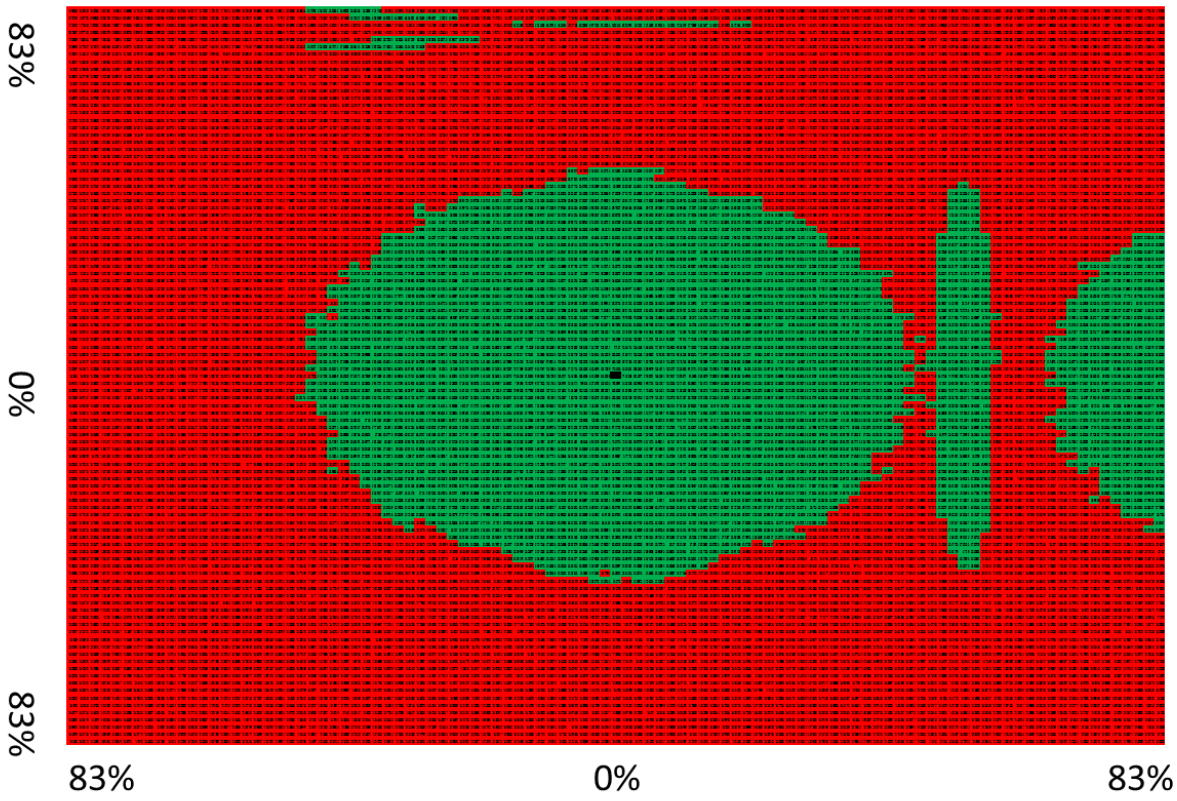

Figure 32: Adjusted acceptable impact region based on continued linear movement of the target at the control speed of 1.02 m/s

The data in this graphic shows an additional area on the righthand side that should be an acceptable region for impact, however this believed to be false and that the region should be symmetrical. The most obvious reason for the inaccuracy is how the batch scenario was setup and calculated. It put additional weight on the y direction in the positive instead of treating both positive and negative equally. For future work, additional examination should be conducted to determine the minimum level of symmetry required for an impact area to be acceptable.

The new acceptable impact area is – 5.6 m to + 5.6 m from the center point, not including the outlier information in both the y and z directions. These dimensions account for 17% of the total area of the net and 46% of each dimension parameter. This shows the need to be within 46% of the radius of the net in order for there to be a successful capture with a target that is significantly

smaller than the net. Future work should look at the effects of different size nets on the same target size and how that impacts the evaluation conducted here with induced angular rates and impact zones.

The next area considered was the change in the target velocity. This area was considered due to the expected variability in the deployment velocity of the bullets from the canister. The results were as expected in that the total distance of the net and target from the chaser at the end of the 300 s scenario is lower with a longer time between capture and drag chute deployment for lower velocities and the opposite for greater velocities. The case of a target traveling at 2 m/s was unsuccessful due to the equivalent velocity of the net vertex only being 1.62 m/s, as seen in Table 8. A subset of the offset analysis was conducted for the new velocities and it showed that at the same offset the target's induced angular rate increased 27%. Also observed was the fact that it took 22% longer for the net and target velocities to equalize. It was initially hypothesized that a target moving slower would be better for chances to catch, however a target that is moving only slightly less than the velocity of the net is best in this case to minimize induced angular momentum.

The next aspect explored was the bullet angle. This was considered due to a possibility of a tipoff angle upon deployment that would change the effective firing angle. The bullet deployment angle analysis only changed the angle of bullet 1, which was the top right bullet as if the observer was looking at the system down the x-axis towards -x. When adjusted from 5 to 10 degrees the range did not show any noticeable impacts on the overall system. The angles were not adjusted to more drastic angles due to the expected hardware constraints of the firing mechanism.

The last area considered for analysis was the bullet velocity. This area was considered due to the likelihood of failures or small differences in friction in one of the bullet firing mechanisms. Each bullet is fired using compressed air that if one leaked between launch and the mission, that bullet would fire at a reduced velocity or not at all. Also considered were velocities greater than expected in case a canister were not monitored and filled correctly and produced more pressure than desired. The test looked at the differences in the velocity of only one bullet between 1 m/s and 5 m/s where 3 m/s was the control case. The velocity of the one bullet was simulated at 0.5 m/s intervals. The remaining three bullets were kept at the control of 3 m/s upon initial firing. The case where one bullet does not fire at all was not simulated, however, was theorized about. If one did not fire and was not released the net would return to strike the chaser after reaching the maximum allowed distance of 28.2 m between two diagonal bullets. A better setup of the system would allow remaining bullets to pull the bullet that was not fired. This case most likely would not capture the target, however it also would not impact the chaser. Future work should take a closer look at this dynamic.

The velocity adjustments were only conducted on the top right bullet as was done for the angle adjustments previously discussed. For a decrease in the velocity of one bullet, it was observed that it induced an angular rate in the target equivalent to an offset of the net. For a 1 m/s velocity of one of the bullets which is -2 m/s off the control case it was noted that the angular rate was equivalent to an offset of +/- 1.8 m in the z and +/- 1.8 m in the y. A change of only -0.5 m/s (2.5 m/s) showed a +/- 0.4 m/s in both directions. These results showed that there was a nonlinear correlation between change in velocity and the equivalent net offset in the induced angular rate. After impact with the target, it was observed that the time to equalize the velocities was less for the greater changes, 12 s when going 1 m/s instead of 18 s when going 3

m/s. The remaining three bullets did increase the velocity of the slower bullet at the cost of some of their own velocity. The overall velocity of the net was lower, but not drastically. The opposite was observed during the case when the velocity of one bullet increased. There was a linear correlation between the velocity change of one bullet and the velocity change of the net vertex. The induced angular rate of the target from the impact shows the same equivalent net offset for the same change in velocity: +/-0.5 m/s showed a +/- 0.4 m/s in both directions. Future research should look at creating more resolution on the impacts of the variable velocity and look to vary all four bullets within a given range simultaneously rather than just one.

Summary

In this chapter, the collected data was analyzed to determine the feasibility of the proposed mission. It was shown that the greatest amount of adjustment to an orbit given the proposed drag chute would be to reduce an 800 km altitude orbit to a lifetime of 7 years. Either a 1000 km altitude orbit needs a larger drag chute or an additional de-orbit propulsion system in order to achieve the desired less than 25 years orbital lifetime. It was determined that an offset of the net when it hits the target has the greatest impact on the likelihood of mission success.

V. Conclusions

Chapter Overview

In this chapter, a very condensed review of the research is presented first. Included are the conclusions of the presented research as well as the significance of the findings. Recommendations for actions to the research community are addressed as well as recommendations for any future work in the area addressed by this research.

Conclusions of Research

Based on the background research presented in Chapter II, it was seen that the issue of space debris is an ever-growing problem. The highest priorities are the sun-synchronous orbits and their associated trash orbits at 89 deg 800 km and 92 deg 1000 km [2]. If 5-10 large debris can be removed from LEO every year it can continue to be used with reduced risk of collision with existing debris. Current projects to remove space debris cover a wide range of applications, however, the main focus for this research is a net and tether concept. A few missions have been proposed with expected launch dates to test some of the developing net and tether technologies using independent satellites.

In Chapter III, the methodology of the research was presented. Covered were the parameters used for the STK lifetime analysis of the expected debris for the orbits of interest. Also explored were the methods used to create the simulation for the proposed concept mission. The primary focus was the defining of the parameters and the equations for the state space modeling of the non-linear problem.

Based on the results presented in Chapter IV, the proposed simulated mission is feasible for a proof of concept mission based on these preliminary analysis. Given the current testing standards for space hardware, concerns raised including the need to be within the center 17% of

the target upon impact is plausible with current technology based on the Level 6 TRL of net and tether system based on the NASA SPHERES mission [42] [43]. The possibility to construct a working system with current technology is also possible based on the background conducted and the currently existing systems using similar hardware designs. The greatest challenge will be incorporating existing hardware within the deployers in the correct configuration.

Based on the research it was also shown that there is a need and there is a possibility to greatly affect targets of interest as presented by the space community. While some targets at the 1000 km altitude orbit may not be feasible for this mission type there are numerous targets at the lower 800 km altitude which would pose the more immediate threat for collisions in the future. If targets are only considered up to 800 km altitude, then only a drag chute would be required for deorbit purposes and no additional propulsion is required.

Overall, the proposed mission appears feasible as a space debris removal mission while the remaining issues of impact accuracy can be significantly reduced by test and further simulations. Also, it is important to note that the control of the target and the chaser is possible based on the LCROSS mission and CubeSat missions that have launched to date [33]. It can work as a secondary mission mounted to an ESPA ring in the proposed configuration if additional ADCS is added to maintain the stability of the chaser during net and/or target deployment.

Significance of Research

The significance of the presented research is a new approach to tackling the problem of active space debris removal. It presents the possibility of being a secondary mission to lower overall debris removal mission costs. Also presented are currently feasible approaches that would not require a significant amount of time to design and test to begin impacting the space

debris problem. A collaboration with some international partners, such as the Surry RemoveDebris Project, could prove a feasible first mission within the next decade.

Recommendations for Action

It is recommended that greater fidelity modeling be conducted on the system that further refines mission parameters. Also, active feedback and control devices should be incorporated into this concept in order to analyze and correct certain parameters of the mission to account for unforeseen circumstances. Some of these devices include distance monitoring of the target and net as well as an ADCS system for the chaser and target.

Recommendations for Future Research

The presented research only scratches the surface of required research that can be conducted in this area. Based on the results and analysis presented several specific opportunities for future work are detailed out below. Some areas of further study are minor, and would only add a small amount of refinement to the problem. However, others are larger would have a greater impact on the mission design. Several of the concepts presented below have been presented previously to facilitate the understanding of some decisions that were made in the progress of the research and are re-iterated here for completeness and ease of reference.

One area of background research includes addressing why going after the largest objects over just those objects with high collision probabilities or damage potentials was the preferable approach. If repeated, the study may focus more on damage potentials from collisions. The proposed analysis would be a simulation and computing intensive effort and may not be a cost-effective approach for mission planning purposes.

Several areas regarding the design of the proposed mission are candidates for future work. One area is to release the drag chute from the chaser before deploying the actual chute. This can be done either before the tether goes taut, or once it goes taut. Based on the results presented, it may be preferable to allow the tether to go taut for an undetermined time before releasing the drag chute. To accomplish this idea, the drag chute would be encased in another small CubeSat such as a 2U, which would deploy independently after a given condition, such as when either a certain time or distance from the chaser had been achieved. If this scenario is explored, additional work is also required into the torque induced on chaser from the target through the tether.

Overall, the simulation can be improved with the inclusion of active feedback control in the modeling to help determine the time required to combat the torques on the chaser and re-align with the target for net deployment. The chaser would also have to combat the torque imparted by the target when the tether goes taut as well as when the bullets are deployed. Additional work into active feedback could be done on the system design allowing the system to adapt to changes in the expected velocities and angles of deployment of the target, bullets and net. Another area of future work would be to improve the resolution of the simulation. The target deployment velocity difference is due to the resolution of the simulation and the time step used in that phase. This also includes modeling the entire deorbit scenario and having the chaser moving in the inertial frame as if it were orbiting, rather than keeping it static in the frame.

Some of the bigger impact areas that require additional work are accounting for the net impacting the target at an angle off center, and what the resulting imparted angular rate would be. Along with the imparted angular rate would be to examine more closely the potential for the target to wind back up the tether after being unwound by the force of the drag chute and chaser.

To conduct this research, higher fidelity for the net and a more refined model that incorporates the flexibility of the net connections, the tether and the drag chute.

In regards to more work on the net itself, if the proposed mission were to be executed, it is recommended that the net be modelled as a more deformable body rather than the rigid body presented in this research. The effects of difference size nets in relation to the same size target should also be explored for planning purposes. The cost benefit analysis should be conducted on the need for accuracy versus weight and likelihood of mission success.

Some areas of the presented research require refinement in future work. The most significant of these is the analysis of net impact mapping. The net mapping presented in relation to the impact offset should be symmetrical, however the results did not show this. Also, refining how the bullets interact to allow for a bullet that was not fired to be dragged along by the other bullets should also be incorporated. The refined model showing how the bullets are dragged in certain cases would be most critical when looking at failure mode analysis. Future research should look at creating more resolution on the impacts of the variable velocity of the bullets and look to vary all four bullets within a given range simultaneously rather than just one. All areas presented for future research are possible next steps in determining the feasibility of the proposed mission.

Summary

In this research, it was theorized that a large piece of space debris could be captured by a net and tether system launched as a secondary mission from a Centaur rocket ESPA ring chaser and deorbited. It has been proven that the theory is feasible given certain constraining parameters. Presented in this chapter was the significance of this research as well as areas for future work related to the presented research and findings.

Bibliography

[1] A. Smith, "20 New Countries to Invest in Space Programs by 2025," Paris, 2016.

[2] J. -C. Liou, "An Active Debris Removal Parametric Study for LEO Environment Remediation," *Advances in Space Research,* vol. 47, pp. 1865-1876, 2011.

[3] M. Shan, J. Guo and E. Gill, "Review and comparison of active space debris capturing and removal methods," *Progress in Aerospace Sciences,* no. 80, pp. 18-32, 2016.

[4] J. R. Wertz, D. F. Everett and J. J. Puschell, Eds., Space Mission Engineering: The New SMAD, Hawthorne, California: Microcosm Press, 2011, p. 208.

[5] R. Benvenuto, S. Salavi and M. Lavagna, "Dynamics analysis and GNC design of flexible systems for space debris removal," *Acta Astronautica*, no. 110, pp. 247-265, 2015.

[6] ESA, "E.DEORBIT," 12 April 2016. [Online]. Available: http://www.esa.int/Our_Activities/Space_Engineering_Technology/Clean_Space/e.Deorbit. [Accessed 20 April 2017].

[7] Aviospace, "CADET (CApture and DE-orbiting Technologies) test campaign video," 23 November 2015. [Online]. Available: http://www.aviospace.com/index.php/news/43-cadetvideo1. [Accessed 9 May 2016].

[8] J. Pelton, "The Space Debris Threat and the Kessler Syndrome," in *Space Debris and Other Threats from Outer Space*, Springer, 2013, pp. 17-23.

[9] M. M. Castronuovo, "Active space debris removal - A preliminary mission analysis and design," *Acta Astronautica*, no. 69, pp. 848-859, 2011.

[10] United Nations, "Technical Report on Space Debris," United Nations Publication, New York, 1999.

[11] M. Schmitz, S. Fasoulas and J. Ultzmann, "Performance Model for Space-Based Laser Debris Sweepers," *Acta Astronautica,* vol. 115, pp. 376-383, 2015.

[12] NASA, "Orbital Debris Improtant Reference Documents," NASA and JSC, 10 August 2010. [Online]. Available: http://orbitaldebris.jsc.nasa.gov/library/references.html. [Accessed 11 April 2016].

[13] NASA, "Space Debris and Human Spacecraft," 26 September 2013. [Online]. Available: http://www.nasa.gov/mission_pages/station/news/orbital_debris.html. [Accessed 9 May 2016].

[14] United Nations Office for Outer Space Affaris, "Space Debris Mitigation Guidelines of the Commitee on the Peaceful Uses of Outer Space," Vienna, 2010.

[15] P. B. de Selding, *Orbital Debris Experts Call for Space Junk Remocal Missions,* 2013.

[16] A. T. Kearsley, G. A. Graham, M. J. Burchell, E. A. Taylor, G. Drolshagen, R. J. Charter and D. McPhail, "MULPEX: A compact multi-layered polymer foil collector for micrometeoroids and orbital debris," *Advances in Space Research,* no. 35, pp. 1270-1281, 2005.

[17] European Space Agency, "Space Debris," 20 April 2013. [Online]. Available: http://www.esa.int/Our_Activities/Operations/Space_Debris/FAQ_Frequently_asked_questions. [Accessed 11 April 2016].

[18] L. Morgan, "Elon Musk Wants to Launch a Fleedt of 4000 Satellites into Low Earth Orbit to Provide Global Internet," 22 September 2015. [Online]. Available: https://nycnews.net/content/283297-elon-musk-wants-launch-fleet-4000-satellites-low-earth-orbit-provide-global-internet. [Accessed 2 May 2016].

[19] German Aeropace Center, "Space Research," 27 June 2011. [Online]. Available: http://www.dlr.de/dlr/en/desktopdefault.aspx/tabid-10196/342_read-265/#/gallery/283. [Accessed 9 May 2016].

[20] K. Yoshida and H. Nakanichi, "The TAKO (Target Collaborativise) Flyer: a New Concept for Future Satellite Servicing," in *6th International Symposium on Artificial Intelligence and Robotics & Automation in Space*, Quebec, 2001.

[21] CADET, "Project Objectives," Aviospace, 2016. [Online]. Available: http://www.aviospace.com/cadet/project-objectives/. [Accessed 9 May 2016].

[22] N. Zinner, A. Williamson, K. Brenner, C. B. John, A. Isaak, M. Knoch, A. Leppek and J. Lestishen, "Junk Hunter: Autonomous Rendezvous, Capture, and De-Orbit of Orbital Debris," in *AIAA Space 2011 Conference & Exposistion*, Long Beach, 2011.

[23] R. Benvenuto and M. R. Lavagna, "Flexible Capture Devices for Medium to Large Debris Active Removal: Simulations Results to Drive Experiments," Research Publications at Politecnico di Milano, Milano, 2013.

[24] F. Zhang and P. Huang, "Segmented control for retrieval of space debris after captured by Tethered Space Robot," IEEE, 28 September 2015. [Online]. Available: http://ieeexplore.ieee.org/xpls/abs_all.jsp?arnumber=7354149&tag=1. [Accessed 9 May 2016].

[25] C. Henry, "NanoRacks to Deploy RemoveDebris Mission from ISS in 2017," 2016.

[26] N. Davis, "Space junk cleanup mission prepars for launch," 2016.

[27] S. Bandyopadhyay, S.-J. Chung and F. Y. Hadaegh, "Nonlinear Attitude Control of Spacecraft with a Large Captured Object," *Journal of Guidance, Control and Dynamics*, vol. 39, no. 4, pp. 754-769, April 2016.

[28] K. Barbaw, "Fishing for Space Junk: New Nets Capture Old Satellites," 10 04 2015. [Online]. Available: http://www.space.com/29070-space-junk-fishing-net-video.html. [Accessed 20 05 2016].

[29] The CubeSat Program, Cal Poly SLO, "Developer Resources," 06 04 2015. [Online]. Available: http://www.cubesat.org/resources/. [Accessed 20 05 2016].

[30] Planetary Systems Corporation, "Canisterized Satellite Dispenser," [Online]. Available: http://www.planetarysystemscorp.com/?post_type=product&p=448. [Accessed 20 05 2016].

[31] ASTRA, "CubeSat Technologies," Virtuallinda Media, [Online]. Available: http://www.astraspace.net/tech-development/cubesat-technologies/. [Accessed 20 05 2016].

[32] H. J. Kramer, "AAReST," 2002. [Online]. Available: https://directory.eoportal.org/web/eoportal/satellite-missions/a/aarest. [Accessed 20 05 2016].

[33] National Aeronautics and Space Administration, "Lunar Reconnaissance Orbiter: Leading NASA's Way Back to the Moon; Lunar Crater Observation and Sensing Satellite: NASA's Mission to Search for Water on the Moon," Huntsville, 2009.

[34] R. Crierie, "Centaur Upper Stage Family," 22 October 2012. [Online]. Available: http://www.alternatewars.com/BBOW/Boosters/Centaur/Centaur.htm. [Accessed 11 January 2017].

[35] "Big Book of Warfare and other stuff," 22 October 2012. [Online]. Available: http://www.alternatewars.com/BBOW/Boosters/Centaur/Centaur.htm. [Accessed 20 April 2017].

[36] Spaceflight , "Spaceflight, Inc. General Payload Users Guide," 22 May 2015. [Online]. Available: http://www.spaceflight.com/wp-content/uploads/2015/05/SPUG-RevF.pdf. [Accessed 20 April 2017].

[37] L. Johnson, "Solar Sail Propulsion," 2012. [Online]. Available: https://ntrs.nasa.gov/archive/nasa/casi.ntrs.nasa.gov/20120015076.pdf.

[38] MathWorks, "ODE45," The MathWorks, Inc., [Online]. Available: https://www.mathworks.com/help/matlab/ref/ode45.html?requestedDomain=www.mathworks.com. [Accessed 24 April 2017].

[39] "How to Calculate Drag in LEO using Matlab," Spacience, 1 March 2012. [Online]. Available: http://spacience.blogspot.com/2012/03/how-to-calculate-drag-in-leo-using.html. [Accessed 3 May 2017].

[40] Systems Tool Kit, "Satellite Lifetime," January 2017. [Online]. Available: http://help.agi.com/stk/index.htm#stk/tools-11.htm. [Accessed 19 January 2017].

[41] E. Swenson, R. Cobb, C. Hartsfield and J. Hess, Interviewees, *Thesis Concpet Initial Orientation.* [Interview]. 11 April 2017.

[42] K. Costello, "International Space Station," NASA, 22 November 2016. [Online]. Available: https://www.nasa.gov/mission_pages/station/reserach/experiments/2182.html. [Accessed 13 May 2017].

[43] B. Dunbar, "Technology Readiness Level," NASA, 31 July 2015. [Online]. Available: https://www.nasa.gov/directorates/heo/scan/engineering/technology/txt_accordion1.html. [Accessed 13 May 2017].

REPORT DOCUMENTATION PAGE		Form Approved OMB No. 074-0188

1. REPORT DATE *(DD-MM-YYYY)*	**2. REPORT TYPE**	**3. DATES COVERED** *(From – To)*
15-06-2017	Master's Thesis	24 Aug 2016 to 15 Jun 2017

4. TITLE AND SUBTITLE
Analysis Of An Experimental Space Debris Removal Mission

5a. CONTRACT NUMBER

5b. GRANT NUMBER

5c. PROGRAM ELEMENT NUMBER

6. AUTHOR(S)

Roth, Krista L, L. Capt, USAF

5d. PROJECT NUMBER
NA

5e. TASK NUMBER

5f. WORK UNIT NUMBER

7. PERFORMING ORGANIZATION NAMES(S) AND ADDRESS(S)
Air Force Institute of Technology
Graduate School of Engineering and Management (AFIT/EN)
2950 Hobson Way, Building 640
WPAFB OH 45433-8865

8. PERFORMING ORGANIZATION REPORT NUMBER
AFIT-ENY-MS-17-J-071

9. SPONSORING/MONITORING AGENCY NAME(S) AND ADDRESS(ES)
None

10. SPONSOR/MONITOR'S ACRONYM(S)

11. SPONSOR/MONITOR'S REPORT NUMBER(S)

12. DISTRIBUTION/AVAILABILITY STATEMENT

DISTRIBUTION STATEMENT A

13. SUPPLEMENTARY NOTES
This material is declared a work of the U.S. Government and is not subject to copyright protection in the United States.

14. ABSTRACT
Encountering space debris is an ever-increasing problem in space exploration and exploitation, especially in Low Earth Orbit. While many space-faring governing bodies have attempted to control the orbital lifetime post mission completion of satellites and rocker bodies, objects already in orbit pose a danger to future mission planning. Currently, governments and academic institutions are working to develop missions to remove space debris; however, the proposed missions are typically costly primary missions. This research proposes an alternative to use an upper stage rocket, to be called a chaser, already launching a primary mission near the desired debris as a host for a removal mission. This research models the alternative system as an experimental test concept deploying a target from the Evolved Expendable Launch Vehicle Secondary Payload Adapter ring. A net and tether system is deployed towards the target to capture it, and at the opposite end of the tether is released a drag chute to deorbit the target. Once the capture method is proven with a cooperative body through experimentation, the target can then be an uncooperative piece of space debris of any size. The orbital life of a dead rocket body in an 800 km sun synchronous orbit can theoretically be reduced from approximately 500 years to less than a year using this method. This proposed concept is new in that it is planned as a secondary mission and the majority of the mission components will not separate from the Payload Adapter ring. This research's initial model predictions show feasibility for this new concept.

15. SUBJECT TERMS
Space Debris, Modeling and Simulation, Net and Tether

16. SECURITY CLASSIFICATION OF:			**17. LIMITATION OF ABSTRACT**	**18. NUMBER OF PAGES**	**19a. NAME OF RESPONSIBLE PERSON**
a. REPORT	**b. ABSTRACT**	**c. THIS PAGE**			Researcher, Eric Swenson, PhD
U	U	U	UU or SAR	95	**19b. TELEPHONE NUMBER** *(Include area code)* (937) 255-6565, x 3329 (eric.swenson@afit.edu)